*Macromolecules* **1993,** *26,* 3663–3675

# Effect of Molecular Weight on the Phase Behavior of Linear and Macrocyclic Oligoethers and of Linear Polyethers Based on 1-(4-Hydroxy-4′-biphenylyl)-2-(4-hydroxyphenyl)butane and 1,10-Dibromodecane[1a]

**Virgil Percec* and Masaya Kawasumi**

*Department of Macromolecular Science, Case Western Reserve University, Cleveland, Ohio 44106-2699*

*Received January 21, 1993; Revised Manuscript Received April 8, 1993*

ABSTRACT: The synthesis and phase behavior of the individual monomer, dimer, trimer, and tetramer, and of the polyethers of 1-(4-hydroxy-4′-biphenylyl)-2-(4-hydroxyphenyl)butane (TPB) with 1,10-dibromodecane (TPB-10) with $M_n$ = 5200 to 57 200, $M_w/M_n$ = 1.16 to 1.47 and with well-defined chain ends are described. The influence of various chain ends on the mesomorphic behavior of monomer and dimer was also discussed. There is a continuous increase of the nematic–isotropic ($T_{ni}$) and glass transition ($T_g$) temperatures over the entire range of molecular weights. The increase of $T_{ni}$ and $T_{in}$ on $M_n$ is very steep up to $M_n$ = 15 000 to 20 000. At higher molecular weights the increase of $T_{ni}$ is much less steep, while $T_{in}$ remains about constant or even decreases slightly. This trend is determined by a continuous increase of the degree of supercooling of the isotropization transition temperature with the increase in molecular weight. Therefore, at low molecular weights the isotropization transition is thermodynamically controlled while at high molecular weights, by analogy with other first-order phase transitions in polymers, it becomes kinetically controlled. $T_g$ determined from both heating and cooling scans follows an identical trend with $T_{ni}$, resulting in a constant $T_{ni}/T_g$ ratio over the entire range of molecular weights. The phase behavior of these linear oligomers and polymers was compared to that of the corresponding macrocyclics reported previously (*Macromolecules* **1992,** *25,* 3851). The macrocyclic trimer, tetramer, and pentamer show isotropization temperatures which are up to 46 °C higher than those of their corresponding linear oligomers and high molecular weight polymers. $T_g$ values of macrocyclics are about 17 °C higher than those of the corresponding linear oligomers. The enthalpy changes associated with the isotropization temperatures of macrocyclics are from 20 up to 2 times lower than those of the linear oligomers and polymers. Also, the crystallization ability of macrocyclics is lower than that of their homologues linear oligomers. This paper provides the most complete set of results on the influence of molecular weight on the phase behavior of linear main chain liquid crystalline polymers and presents the first study which compares the phase behavior of macrocyclics with that of the their corresponding linear architectures.

## Introduction

The elucidation of the influence of molecular weight on the phase behavior and on the dynamics and the physical properties of liquid crystalline polymers represents one of the most basic and important subjects which has both theoretical and practical implications for the entire field. Molecular weight is responsible for the transition from molecular to macromolecular liquid crystals and, therefore, generates all differences and similarities between them. At the most elemental level, molecular weight influences all thermal transition temperatures and their associated thermodynamic parameters as well as the relative thermodynamic stabilities of various phases. This dependence was recently discussed based on basic thermodynamic principles and the predicted trends were compared with experimental data available in the literature.[1b–e]

In the case of side chain liquid crystalline polymers there are quite comprehensive series of investigations on this topic.[2] Preparation of side-chain liquid crystalline polymers with well-defined molecular weight and chain ends and with narrow molecular weight distribution was first made possible by using fractionation methods.[2a–c] However, recently the application of various living polymerization techniques to mesogenic monomers such as group transfer polymerization of methacrylates,[2d] cationic polymerization of vinyl ethers,[2e] and ring opening metathesis polymerization of cyclic olefins[2f] have contributed to the development of both reliable data and suitable techniques and systems for these investigations.

In contrast to side chain liquid crystalline polymers which are synthesized mostly by chain polymerization reactions,[2a] main chain liquid crystalline polymers are prepared by step polymerization reactions.[1d] Step polymerization reactions lead to polymers with broad polydispersity containing both linear and cyclic macromolecules and, therefore, a combination of individual oligomeric model compounds and fractionated samples of higher molecular weight polymers from which the cyclic oligomers were separated is required for such a quantitative investigation. The most comprehensive investigation on main chain liquid crystalline polyesters in which both monomeric and dimeric model compounds and fractionated polymers with number average molecular weights from 700 to 19 000 was provided by Blumstein et al.[3] Their work has generated the first series of results which elucidated the influence of molecular weight and chain ends on thermal transition temperatures and thermodynamic parameters. Additional examples of experiments on the influence of molecular weight on phase transitions without using low molecular weight model compounds are available.[4–7] Although it is well established that individual oligomers are excellent models for the corresponding polymers, mostly dimers were synthesized and investigated so far.[8] This limitation was generated by the low solubility of the oligomeric model compounds and of their high molecular weight homologues.

---

* To whom all correspondence should be addressed.

0024-9297/93/2226-3663$04.00/0

**Scheme I. Synthesis of Linear TPB-10 Monomer and Dimer**

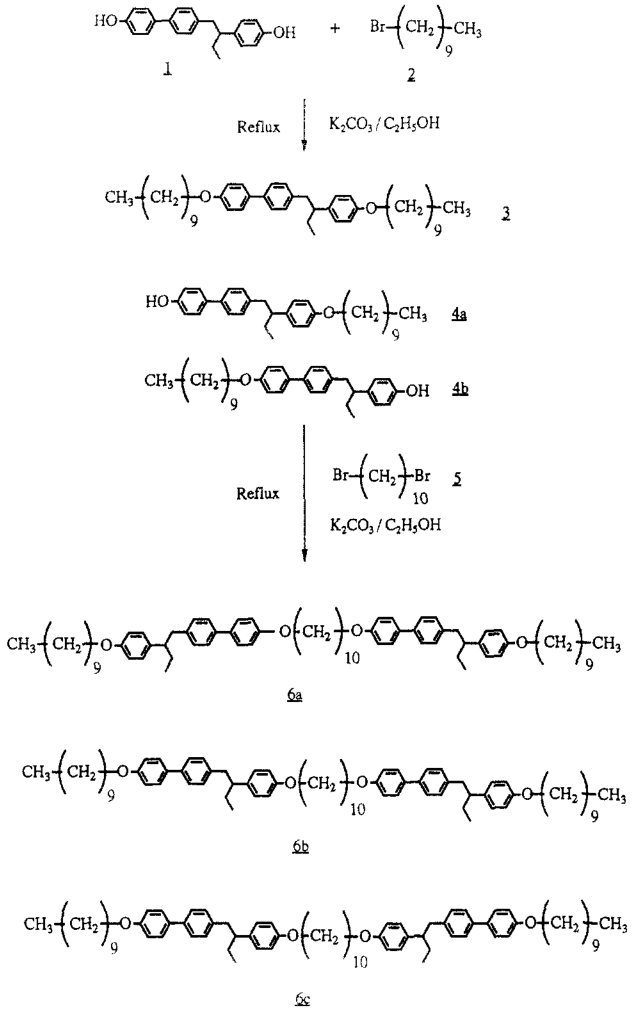

**Scheme II. Synthesis of Linear TPB-10 Trimer**

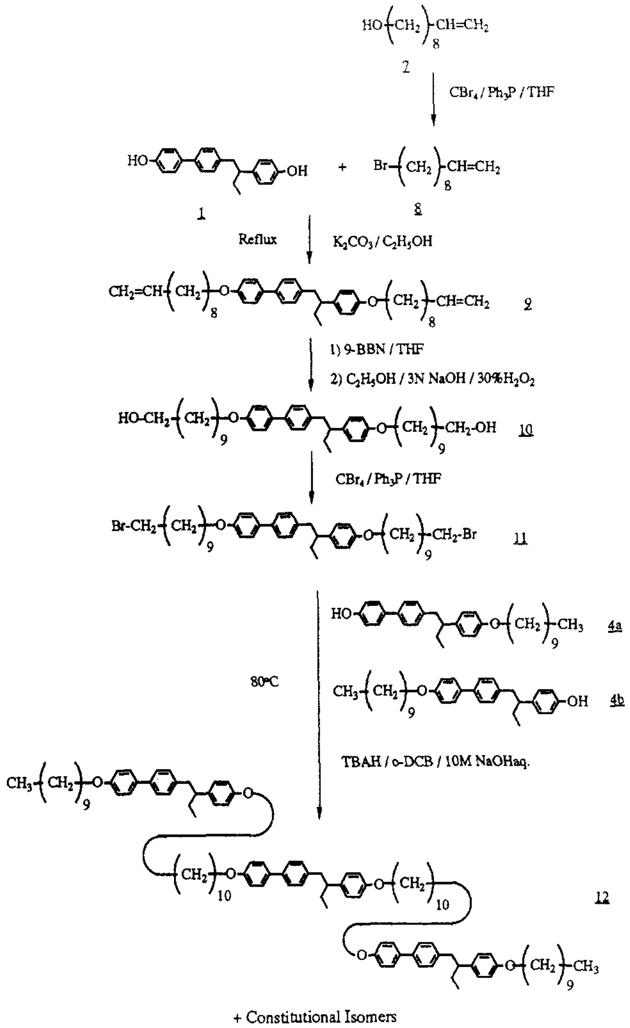

Recently, we have elaborated the synthesis of racemic[9] and chiral[10] 1-(4-hydroxy-4′-biphenylyl)-2-(4-hydroxyphenyl)butane (TPB) and reported the synthesis and characterization of linear polyethers[9,10] and of low and high molecular weight macrocyclics[11] of TPB with $\alpha,\omega$-dibromoalkanes. The first examples of dendrimeric liquid crystalline polymers were also reported by elaborating $AB_2$ monomers related to TPB.[12] All these oligomers and polymers are soluble in conventional solvents and are presently used as models for various dynamic and physical investigations.[13]

The first goal of this paper is to present the elaboration of synthetic methods for the preparation of linear model compounds (i.e., monomer, dimer, trimer, and tetramer) with various chain ends, and of high molecular weight linear polyethers with narrow molecular weight distribution and well-defined chain ends ($M_n$ = 5200 to 57 200; $M_n/M_w$ = 1.16 to 1.47) based on TPB and 1,10-dibromodecane (TPB-10). The second goal is to discuss the influence of molecular weight on the mesomorphic behavior of linear TPB-10. The third goal is to compare the mesomorphic behavior of linear and macrocyclic oligomers. To our knowledge, this report provides the most complete series of data on the influence of molecular weight on the phase behavior of main chain liquid crystalline oligomers and polymers and the first comparison between the phase behavior of macrocyclic and linear oligomers.

## Experimental Section

**Materials.** 1-Bromodecane (98%), $CBr_4$ (99%), $PPh_3$ (99%), tetrabutylammonium hydrogen sulfate (TBAH, 97%), 9-BBN [0.5 M solution in tetrahydrofuran (THF)], 9-decen-1-ol (98%) (all from Aldrich), potassium carbonate, and 30% $H_2O_2$ (both from Fisher Scientific) were used as received. 1,10-Dibromodecane (97%) (from Aldrich) was purified by vacuum distillation. THF was dried by refluxing over $LiAlH_4$ followed by distillation. *o*-Dichlorobenzene was distilled under reduced pressure. All other chemicals were commercially available and were used as received. TPB (99.9%) was synthesized according to the previously described procedure.[9]

**Synthesis of Linear TPB-10 Oligomers.** The synthetic routes used in the preparation of linear TPB-10 oligomers are described in Schemes I–III.

**Synthesis of Linear TPB-10 Monomer (3) and of Monodecyl-TPB (4a and 4b).** **3**, **4a**, and **4b** were prepared by the etherification of TPB (**1**) with 1-bromodecane (**2**). TPB (1.91 g, 6.0 mmol) was dissolved in 30 mL of absolute ethanol in a 100-mL one-neck flask equipped with reflux condenser and magnetic stirrer. After anhydrous $K_2CO_3$ (0.83 g, 6.0 mmol) was added, the reaction mixture was stirred under nitrogen atmosphere at reflux temperature for 1.5 h. 1-Bromodecane (1.33 g, 6.0 mmol) was added and the reaction mixture was stirred at reflux temperature for 24 h. After evaporation of the ethanol the remaining solid was dissolved in 50 mL of $CHCl_3$. The organic layer was washed with water, dilute aqueous HCl, and water, dried over anhydrous $MgSO_4$, and filtered. The solvent was evaporated to yield a solid which contained TPB-10 monomer, monodecyl-TPB, and TPB. This mixture was separated into monodecyl-TPB and TPB-10 monomer by silica gel column chromatography using a mixture of hexanes and diethyl ether (3:1) as eluent to yield 1.04 g (37.8%) of monodecyl-TPB and 0.589 g (16.4%) of TPB-10 monomer. Purity (HPLC): monodecyl-TPB, >99%; TPB-10 monomer, >99%. $^1H$ NMR of monodecyl-TPB ($CDCl_3$, TMS, $\delta$, ppm): 0.77 (3H, Ph-CH-$CH_2$-$CH_3$, t, $J$ = 7.7 Hz), 0.89 (3H, -O-$(CH_2)_9$-$CH_3$, t, $J$ = 6.3 Hz), 1.28 (14H, $CH_3$-$(CH_2)_7$-, m), 1.63 (2H, Ph-CH-$CH_2$-$CH_3$, m), 1.76

Scheme III. Synthesis of Linear TPB-10 Tetramer

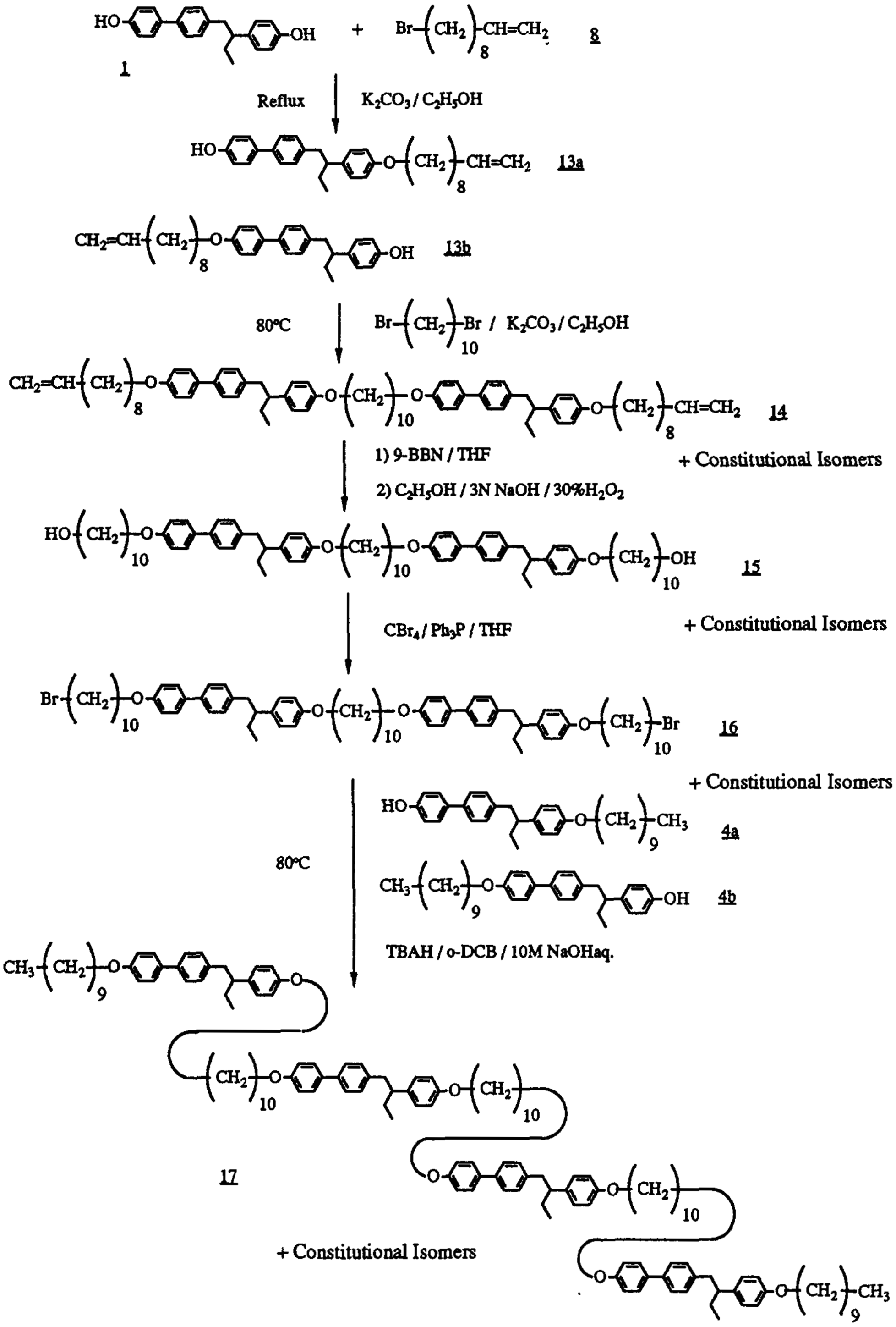

(2H, –O–CH$_2$–C*H*$_2$–, m), 2.68 (1H, Ph–C*H*–, m), 2.86 (2H, Ph–C*H*$_2$–CH–, d, *J* = 7.6 Hz), 3.92 and 3.98 (2H, –O–C*H*$_2$–, 2t), 4.67 and 4.88 (1H, –O*H*, 2s), 6.74 and 6.81 (2H, ortho to hydroxy or ether of the monophenyl ring, 2d, *J* = 8.5 and 8.3 Hz), 6.87 and 6.94 (2H, ortho to hydroxy or ether of the biphenyl ring, 2d, *J* = 8.5 and 9.3 Hz), 6.99 (2H, ortho to methine of the monophenyl ring, d, *J* = 9.3 Hz), 7.06 (2H, ortho to methylene of the biphenyl ring, d, *J* = 7.9 Hz), 7.40 (2H, meta to methylene of the biphenyl ring, d, *J* = 8.4 Hz), 7.48 (2H, meta to hydroxy or ether of the biphenyl ring, d, *J* = 8.5 Hz). The ratio of **4b** to **4a** was 79/21. $^1$H NMR of TPB-10 monomer (CDCl$_3$, TMS, δ, ppm): 0.76 (3H, Ph–CH–CH$_2$–C*H*$_3$, t, *J* = 7.5 Hz), 0.88 (6H, –O–(CH$_2$)$_9$–C*H*$_3$, t, *J* = 6.3 Hz), 1.27 (28H, CH$_3$–(C*H*$_2$)$_7$–, m), 1.63 (2H, Ph–CH–C*H*$_2$–CH$_3$, m), 1.76 (4H, –O–CH$_2$–C*H*$_2$–, m), 2.68 (1H, Ph–C*H*–, m), 2.86 (2H, Ph–C*H*$_2$–CH–, d, *J* = 7.3 Hz), 3.90 (2H, monophenyl–O–C*H*$_2$–, t, *J* = 6.2 Hz), 3.98 (2H, biphenyl–O–C*H*$_2$–, t, *J* = 6.4 Hz), 6.81 (2H, ortho to ether of the monophenyl ring, d, *J* = 8.2 Hz), 6.95 (2H, ortho to ether of the biphenyl ring, d, *J* = 7.2 Hz), 7.03 (2H, ortho to methine of the monophenyl ring, d, *J* = 7.4 Hz), 7.07 (2H, ortho to methylene of the biphenyl ring, d, *J* = 7.3 Hz), 7.40 (2H, meta to methylene of the biphenyl ring, d, *J* = 8.6 Hz), 7.48 (2H, meta to ether of the biphenyl ring, d, *J* = 8.8 Hz).

**Synthesis of Linear TPB-10 Dimer (6).** **6** was prepared by the etherification of monodecyl-TPB (**4a** and **4b**) with 1,10-dibromodecane (**5**) using a similar procedure to the one used for **4a** and **4b** with the following modifications. **4a** and **4b** (0.298 g, 0.65 mmol), 10 mL of absolute ethanol, anhydrous K$_2$CO$_3$ (0.099 g, 0.715 mmol), and 1,10-dibromodecane (0.098 g, 0.325 mmol) was used. The total reaction time was 23 h. The reaction mixture was worked up by using a similar procedure to the one used for **4a** and **4b**. The resulting product was purified twice by silica gel column chromatography using a mixture of hexanes and diethyl ether (first 4:1, second 20:1) as eluent to yield 0.131 g (38.1%) of linear TPB-10 dimer. Purity (HPLC): >99%. $^1$H NMR (CDCl$_3$, TMS, δ, ppm): 0.76 (6H, Ph–CH–CH$_2$–C*H*$_3$, t, *J* = 7.4

Hz), 0.88 (6H, $-\mathrm{O}-(\mathrm{CH_2})_9-\mathrm{C}H_3$, t, $J = 5.9$ Hz), 1.27 (28H, $\mathrm{CH_3}-(\mathrm{C}H_2)_7-$, m), 1.33 (12H, $-\mathrm{O}-\mathrm{CH_2}-\mathrm{CH_2}-(\mathrm{C}H_2)_6-$, m), 1.63 (4H, $\mathrm{Ph}-\mathrm{CH}-\mathrm{C}H_2-\mathrm{CH_3}$, m), 1.76 (8H, $-\mathrm{O}-\mathrm{CH_2}-\mathrm{C}H_2-$, m), 2.68 (2H, $\mathrm{Ph}-\mathrm{C}H-$, m), 2.87 (4H, $\mathrm{Ph}-\mathrm{C}H_2-\mathrm{CH}-$, d, $J = 6.5$ Hz), 3.92 (4H, monophenyl–$\mathrm{O}-\mathrm{C}H_2-$, t, $J = 5.8$ Hz), 3.98 (4H, biphenyl–$\mathrm{O}-\mathrm{C}H_2-$, t, $J = 6.7$ Hz), 6.81 (4H, ortho to ether of the monophenyl ring, d, $J = 8.3$ Hz), 6.94 (4H, ortho to ether of the biphenyl ring, d, $J = 8.5$ Hz), 7.03 (4H, ortho to methine of the monophenyl ring, d, $J = 7.7$ Hz), 7.07 (4H, ortho to methylene of the biphenyl ring, d, $J = 7.0$ Hz), 7.40 (4H, meta to methylene of the biphenyl ring, d, $J = 8.0$ Hz), 7.48 (4H, meta to ether of the biphenyl ring, d, $J = 9.0$ Hz).

**Synthesis of 1-Bromo-9-decene (8).** 1-Bromo-9-decene (8) was synthesized by the bromination of 9-decene-1-ol (7) with $\mathrm{CBr_4}$ and $\mathrm{PPh_3}$.[14] 9-Decene-1-ol (12.5 g, 80 mmol) and carbon tetrabromide (33.2 g, 100 mmol) were dissolved in dry THF in a 50-mL three-neck flask equipped with addition funnel, nitrogen inlet–outlet, and magnetic stirrer. A solution of triphenylphosphine (26.2 g, 100 mmol) in dry THF (500 mL) was added dropwise to the reaction mixture under cooling with an ice–water bath. The color of the reaction mixture changed to yellow and a precipitate occurred. The reaction mixture was stirred at room temperature for 4.5 h. The precipitate was removed by filtration and washed with THF. After the evaporation of THF, the product was extracted with about 300 mL of hexanes followed by the evaporation of hexanes. The resulting liquid was distilled 2 times under vacuum to yield a colorless liquid (14.0 g, 80.0%), bp 55–59 °C (0.55 mmHg). $^1$H NMR ($\mathrm{CDCl_3}$, TMS, $\delta$, ppm): 1.31 (12H, $\mathrm{Br}-\mathrm{CH_2}-(\mathrm{C}H_2)_6-$, m), 1.86 (2H, $\mathrm{Br}-\mathrm{CH_2}-\mathrm{C}H_2-$, m), 2.05 (2H, $-\mathrm{C}H_2-\mathrm{CH}{=}\mathrm{CH_2}$, m), 3.43 (2H, $\mathrm{Br}-\mathrm{C}H_2-$, t, $J = 6.8$ Hz), 4.96 (2H, $-\mathrm{CH}{=}\mathrm{C}H_2$, m), 5.83 (1H, $-\mathrm{C}H{=}\mathrm{CH_2}$, m).

**Synthesis of Didecenyl-TPB-10 Monomer (9).** 9 was prepared by the etherification of TPB (1) with 1-bromo-9-decene (8) by using a similar procedure to the one used for **4a** and **4b**. TPB (3.18 g, 10 mmol), 50 mL of absolute ethanol, anhydrous $\mathrm{K_2CO_3}$ (4.15 g, 30 mmol) and 1-bromo-9-decene (5.26 g, 24 mmol) were used. The etherification was carried out for 23 h. The reaction mixture was worked up by using a similar procedure to the one used for **4a** and **4b**. The product was purified twice by silica gel column chromatography (first with hexanes, second with a mixture of hexanes and diethyl ether (4:1) as eluent) to yield 4.56 g (76.6%) or didecenyl-TPB-10 monomer (**9**). Purity (HPLC): >99%. $^1$H NMR ($\mathrm{CDCl_3}$, TMS, $\delta$, ppm): 0.77 (3H, $\mathrm{Ph}-\mathrm{CH}-\mathrm{CH_2}-\mathrm{C}H_3$, t, $J$ - 7.3 Hz), 1.33 (20H, $-(\mathrm{C}H_2)_5-\mathrm{CH_2}-\mathrm{CH}{=}\mathrm{CH_2}$, m), 1.76 (6H, $\mathrm{Ph}-\mathrm{O}-\mathrm{CH_2}-\mathrm{C}H_2-$ and $\mathrm{Ph}-\mathrm{CH}-\mathrm{C}H_2-\mathrm{CH_3}$, m), 2.03 (4H, $-\mathrm{C}H_2-\mathrm{CH}{=}\mathrm{CH_2}$, m), 2.69 (1H, $\mathrm{Ph}-\mathrm{C}H-$, m), 2.87 (2H, $\mathrm{Ph}-\mathrm{C}H_2-\mathrm{CH}-$, d, $J = 6.8$ Hz), 3.92 (2H, monophenyl–$\mathrm{O}-\mathrm{C}H_2-$, t, $J = 6.3$ Hz), 3.99 (2H, biphenyl–$\mathrm{O}-\mathrm{C}H_2-$, t, $J = 6.7$ Hz), 4.96 (4H, $-\mathrm{CH}{=}\mathrm{C}H_2$, m), 5.81 (2H, $-\mathrm{C}H{=}\mathrm{CH_2}$, m), 6.81 (2H, ortho to ether of the monophenyl ring, d, $J = 8.3$ Hz), 6.94 (2H, ortho to ether of the biphenyl ring, d, $J = 8.2$ Hz), 7.04 (2H, ortho to methine of the monophenyl ring, d, $J = 7.6$ Hz), 7.08 (2H, ortho to methylene of the biphenyl ring, d, $J = 7.4$ Hz), 7.40 (2H, meta to methylene of the biphenyl ring, d, $J = 7.2$ Hz), 7.49 (2H, meta to ether of the biphenyl ring, d, $J = 7.9$ Hz).

**Synthesis of Dihydroxydecyl-TPB-10 Monomer (10).** Monomer **10** was prepared by the hydroboration of monomer **9** according to a literature procedure.[15] Monomer **9** (4.50 g, 7.56 mmol) was dissolved in 10 mL of dry THF in a 100-mL three-neck flask equipped with addition funnel, magnetic stirrer, and nitrogen inlet–outlet. 9-BBN (0.5 M THF solution, 39.4 mL, 19.7 mmol) was added dropwise to the solution after which the reaction mixture was stirred at room temperature for 3 h under nitrogen atmosphere. The organoborane was treated with 12 mL of ethanol followed by 8 mL of 3 N NaOH. $\mathrm{H_2O_2}$ (30%) (8.0 mL) was added dropwise slowly so that the temperature was maintained below 50 °C. The reaction mixture was further stirred at 50 °C for 1 h, cooled, and extracted with 100 mL of diethyl ether twice. The extract was washed 2 times with water and was dried over anhydrous $\mathrm{MgSO_4}$. After evaporation of the solvents, the resulting solid was purified by silica gel column chromatography with hexanes and diethyl ether (3:1) as eluent to yield 3.70 g (yield, 77.5%) of a white solid. Purity (HPLC), 97.7%. $^1$H NMR ($\mathrm{CDCl_3}$, TMS, $\delta$, ppm): 0.76 (3H, $\mathrm{Ph}-\mathrm{CH}-\mathrm{CH_2}-\mathrm{CH_3}$, t, $J = 7.1$ Hz), 1.32 (24H, $\mathrm{HO}-(\mathrm{CH_2})_2-(\mathrm{C}H_2)_6-$, m), 1.56 (6H, $\mathrm{HO}-\mathrm{CH_2}-\mathrm{C}H_2-$ and $\mathrm{Ph}-\mathrm{CH}-\mathrm{C}H_2-\mathrm{CH_3}$, m), 1.76 (4H, $\mathrm{Ph}-\mathrm{O}-\mathrm{CH_2}-\mathrm{C}H_2-$, m), 2.69 (1H, $\mathrm{Ph}-\mathrm{C}H-$, m), 2.87 (2H, $\mathrm{Ph}-\mathrm{C}H_2-\mathrm{CH}-$, d, $J = 7.4$ Hz), 3.64 (4H, $\mathrm{HO}-\mathrm{C}H_2-$, t, $J = 6.3$ Hz), 3.92 (2H, monophenyl–$\mathrm{O}-\mathrm{C}H_2-$, t, $J = 6.3$ Hz), 3.98 (2H, biphenyl–$\mathrm{O}-\mathrm{C}H_2-$, t, $J = 6.5$ Hz), 6.81 (2H, ortho to ether of the monophenyl ring, d, $J = 8.1$ Hz), 6.94 (2H, ortho to ether of the biphenyl ring, d, $J = 7.2$ Hz), 7.03 (2H, ortho to methine of the monophenyl ring, d, $J = 7.6$ Hz), 7.07 (2H, ortho to methylene of the biphenyl ring, d, $J = 7.5$ Hz), 7.40 (2H, meta to methylene of the biphenyl ring, d, $J = 7.1$ Hz), 7.49 (2H, meta to methylene of the biphenyl ring, d, $J = 8.5$ Hz).

**Synthesis of Dibromodecyl-TPB-10 Monomer (11).** **11** was synthesized by a similar method to the one used for **8** except for the following conditions. Monomer **10** (3.46 g, 5.5 mmol), $\mathrm{CBr_4}$ (4.38 g, 13.2 mmol), $\mathrm{PPh_3}$ (3.46 g, 13.2 mmol), and dry THF (100 mL for $\mathrm{CBr_4}$, 15 mL for $\mathrm{PPh_3}$) were used. The reaction time was 3 h. The reaction mixture was worked up by using a similar procedure to the one used for **8**. The resulting product was purified by silica gel column chromatography 2 times. First, only hexanes was used as eluent to remove excess of $\mathrm{CBr_4}$. A mixture of hexanes and diethyl ether (1:1) was then used. The evaporation of the solvent yielded a colorless liquid (3.43 g, 82.4%) which solidified on standing. Purity (HPLC), 97.3%. $^1$H NMR ($\mathrm{CDCl_3}$, TMS, $\delta$, ppm): 0.76 (3H, $\mathrm{Ph}-\mathrm{CH}-\mathrm{CH_2}-\mathrm{C}H_3$, t, $J = 7.2$ Hz), 1.32 (24H, $\mathrm{Br}-(\mathrm{CH_2})_2-(\mathrm{C}H_2)_6-$, m), 1.56 (2H, $\mathrm{Ph}-\mathrm{CH}-\mathrm{C}H_2-\mathrm{CH_3}$, m), 1.82 (8H, $\mathrm{Br}-\mathrm{CH_2}-\mathrm{C}H_2-$ and $\mathrm{Ph}-\mathrm{O}-\mathrm{CH_2}-\mathrm{C}H_2-$, m), 2.68 (1H, $\mathrm{Ph}-\mathrm{C}H-$, m), 2.87 (2H, $\mathrm{Ph}-\mathrm{C}H_2-\mathrm{CH}-$, d, $J = 7.0$ Hz), 3.41 (4H, $\mathrm{Br}-\mathrm{C}H_2-$, t, $J = 6.8$ Hz), 3.92 (2H, monophenyl–$\mathrm{O}-\mathrm{C}H_2-$, t, $J = 6.3$ Hz), 3.98 (2H, biphenyl–$\mathrm{O}-\mathrm{C}H_2-$, t, $J = 6.4$ Hz), 6.81 (2H, ortho to ether of the monophenyl ring, d, $J = 8.4$ Hz), 6.94 (2H, ortho to ether of the biphenyl ring, d, $J = 8.7$ Hz), 7.04 (2H, ortho to methine of the monophenyl ring, d, $J = 7.8$ Hz), 7.07 (2H, ortho to methylene of the biphenyl ring, d, $J = 6.9$ Hz), 7.40 (2H, meta to methylene of the biphenyl ring, d, $J = 8.0$ Hz), 7.49 (2H, meta to ether of the biphenyl ring, d, $J = 9.4$ Hz).

**Synthesis of Linear TPB-10 Trimer (12).** The TPB-10 trimer (**12**) was synthesized by the etherification of dibromodecyl-TPB-10 monomer (**11**) with monodecyl-TPB (**4a, 4b**). To a 25-mL single-neck flask equipped with condenser and magnetic stirrer were added successively monodecyl-TPB (0.321 g, 0.70 mmol), 3.0 mL of 10 N NaOH aqueous solution (30 mmol), 3.0 mL of *o*-dichlorobenzene, dibromodecyl-TPB-10 monomer (0.265 g, 0.35 mmol), and TBAH (0.095 g, 0.28 mmol). A balloon filled with nitrogen was placed at the top of the condenser. The reaction mixture was stirred with 1100 rpm at 80 °C. After 50 min, the reaction mixture was diluted with water and chloroform, and the aqueous layer was removed. The organic layer was washed with water, followed by dilute aqueous HCl, and 2 times with water. The product was precipitated in methanol. The product was first dried under vacuum and then was purified by silica gel column chromatography with a mixture of hexanes and diethyl ether (10:1) as eluent to yield a white solid (0.338 g, 63.8%). Purity (HPLC), >99%. $^1$H NMR ($\mathrm{CDCl_3}$, TMS, $\delta$ ppm): 0.76 (9H, $\mathrm{Ph}-\mathrm{CH}-\mathrm{CH_2}-\mathrm{C}H_3$, t, $J = 7.2$ Hz), 0.88 (6H, $-\mathrm{O}-(\mathrm{CH_2})_9-\mathrm{C}H_3$, t, $J = 6.3$ Hz), 1.27 and 1.33 (52H, $\mathrm{CH_3}-(\mathrm{C}H_2)_7-$ and $-\mathrm{O}-\mathrm{CH_2}-\mathrm{CH_2}-(\mathrm{C}H_2)_6-$, m), 1.63 (6H, $\mathrm{Ph}-\mathrm{CH}-\mathrm{C}H_2-\mathrm{CH_3}$, m), 1.76 (12H, $-\mathrm{O}-\mathrm{CH_2}-\mathrm{C}H_2-$, m), 2.68 (3H, $\mathrm{Ph}-\mathrm{C}H-$, m), 2.87 (6H, $\mathrm{Ph}-\mathrm{C}H_2-\mathrm{CH}-$, d, $J = 7.3$ Hz), 3.92 (6H, monophenyl–$\mathrm{O}-\mathrm{C}H_2-$, t, $J = 6.0$ Hz), 3.98 (6H, biphenyl–$\mathrm{O}-\mathrm{C}H_2-$, t, $J = 6.2$ Hz), 6.80 (6H, ortho to ether of the monophenyl ring, d, $J = 8.0$ Hz), 6.93 (6H, ortho to ether of the biphenyl ring, d, $J = 8.3$ Hz), 7.03 (6H, ortho to methine of the monophenyl ring, d, $J = 7.9$ Hz), 7.07 (6H, ortho to methylene of the biphenyl ring, d, $J = 7.4$ Hz), 7.39 (6H, meta to methylene of the biphenyl ring, d, $J = 7.9$ Hz), 7.48 (6H, meta to ether of the biphenyl ring, d, $J = 8.3$ Hz).

**Synthesis of Monodecenyl-TPB (13a, 13b).** The mixture of **13a** with **13b** was prepared by the etherification of TPB (1) with 1-bromo-9-decene (8) using the same method as that used for **4a** and **4b**. TPB (2.55 g, 8.0 mmol), 40 mL of absolute ethanol, anhydrous $\mathrm{K_2CO_3}$ (1.11 g, 8.0 mmol), and 1-bromo-9-decene (1.76 g, 8.0 mmol) were used. The etherification was carried out for 14.5 h. The reaction mixture was worked up by using a similar procedure to the one used for **4a** and **4b**. The mixture of **13a** with **13b** was separated from the reaction mixture by silica gel column chromatography with a mixture of hexanes and diethyl ether (3:1) as eluent. Evaporation of the solvent yielded 1.68 g (46.0%) of white crystals. Purity (HPLC), >99%. $^1$H NMR ($\mathrm{CDCl_3}$, TMS, $\delta$, ppm): 0.77 (3H, $\mathrm{Ph}-\mathrm{CH}-\mathrm{CH_2}-\mathrm{C}H_3$, t, $J = 7.4$ Hz), 1.33 (12H, $\mathrm{CH_2}{=}\mathrm{CH}-(\mathrm{C}H_2)_6-$, m), 1.63 (2H, $\mathrm{Ph}-\mathrm{CH}-\mathrm{C}H_2-$

CH$_3$, m), 1.76 (2H, –O–CH$_2$–C$H_2$–, m), 2.04 (2H, CH$_2$=CH–C$H_2$–, m), 2.68 (1H, Ph–C$H$–, m), 2.86 (2H, Ph–C$H_2$–CH–, d, $J$ = 6.1 Hz), 3.92 and 3.98 (2H, –O–CH$_2$–, 2t), 4.69 and 4.88 (1H, –O$H$, 2s), 4.76 (2H, C$H_2$=CH–, m), 5.82 (1H, CH$_2$=C$H$–, m), 6.74 and 6.81 (2H, ortho to hydroxy or ether of the monophenyl ring, 2d, $J$ = 8.2 and 8.3 Hz), 6.87 and 6.94 (2H, ortho to hydroxy or ether of the biphenyl ring, 2d, $J$ = 8.4 and 9.6 Hz), 6.99 (2H, ortho to methine of the monophenyl ring, d, $J$ = 9.5 Hz), 7.06 (2H, ortho to methylene of the biphenyl ring, d, $J$ = 7.6 Hz), 7.39 (2H, meta to methylene of the biphenyl ring, d, $J$ = 8.0 Hz), 7.48 (2H, meta to hydroxy or ether of the biphenyl ring, d, $J$ = 8.0 Hz). The ratio of **13b** to **13a** could not be determined due to the severe overlapping.

**Synthesis of Didecenyl-TPB-10 Dimer (14).** Dimer **14** was synthesized by the etherification of 1,10-dibromodecane (**5**) with the mixture of **13a** and **13b** using a similar method to the one used for **12** except the following conditions. **13a** and **13b** (0.709 g, 1.55 mmol), 3.1 mL of 10 N NaOH aqueous solution (31 mmol), 3.1 mL of *o*-dichlorobenzene, 1,10-dibromodecane (0.225 g, 0.75 mmol), and TBAH (0.132 g, 0.39 mmol) were used. The reaction time was 75 min. After working up by the same method as that used for **12**, the product was precipitated in methanol and dried under vacuum. A final purification by silica gel column chromatography with a mixture of hexane and diethyl ether (3:1) as eluent followed by the evaporation of solvents yielded a white solid (0.653 g, 82.7%). Purity (HPLC), >99%. $^1$H NMR (CDCl$_3$, TMS, $\delta$, ppm): 0.76 (6H, Ph–CH–CH$_2$–C$H_3$, t, $J$ = 7.1 Hz), 1.33 (32H, Ph–O–(CH$_2$)$_2$–(C$H_2$)$_6$–(CH$_2$)$_2$–O–Ph and –(C$H_2$)$_5$–CH=CH$_2$, m), 1.76 (12H, Ph–O–CH$_2$–C$H_2$– and Ph–CH–C$H_2$–CH$_3$, m), 2.05 (4H, –C$H_2$–CH=CH$_2$, m), 2.69 (2H, Ph–C$H$–, m), 2.86 (4H, Ph–C$H_2$–CH–, d, $J$ = 7.3 Hz), 3.92 (4H, monophenyl–O–C$H_2$–, t, $J$ = 6.1 Hz), 3.98 (4H, biphenyl–O–C$H_2$–, t, $J$ = 6.3 Hz), 4.96 (4H, –CH=C$H_2$, m), 5.82 (2H, –C$H$=CH$_2$, m), 6.81 (4H, ortho to ether of the monophenyl ring, d, $J$ = 8.3 Hz), 6.94 (4H, ortho to ether of the biphenyl ring, d, $J$ = 8.6 Hz), 7.04 (4H, ortho to methine of the monophenyl ring, d, $J$ = 7.3 Hz), 7.07 (4H, ortho to methylene of the biphenyl ring, d, $J$ = 6.6 Hz), 7.40 (4H, meta to methylene of the biphenyl ring, d, $J$ = 7.1 Hz), 7.48 (4H, meta to ether of the biphenyl ring, d, $J$ = 8.1 Hz).

**Synthesis of Dihydroxydecyl-TPB-10 Dimer (15).** **15** was prepared by a similar procedure to the one used for **10** except for the following conditions. Dimer 14 (0.631 g, 0.60 mmol) was dissolved in a 4.8 mL of dry THF. 9-BBN (0.5 M THF solution, 4.8 mL, 2.4 mmol) was added dropwise to the solution after which the reaction mixture was stirred at room temperature for 6 h under nitrogen atmosphere. The organoborane was treated with 1.8 mL of ethanol followed by 1.1 mL of 3 N NaOH. H$_2$O$_2$ (30%) (1.1 mL) was added dropwise. The reaction mixture became cloudy during the addition of H$_2$O$_2$ solution. A few milliliters of THF was added to the reaction mixture to maintain it homogeneous. The reaction was further stirred at 50 °C for 1.5 h, cooled, and extracted with 50 mL of CHCl$_3$. The extract was washed 3 times with water and than was dried over anhydrous MgSO$_4$. After the filtration and evaporation of the solvents, the resulting solid was purified 3 times by silica gel column chromatography with mixtures of petroleum ether and diethyl ether (first, 1:1, second, 2:1, third, 3:1) as eluent followed by the evaporation of solvents to yield 0.448 g (68.7%) of a white solid. Purity (HPLC), >99%. $^1$H NMR (CDCl$_3$, TMS, $\delta$, ppm): 0.76 (6H, Ph–CH–CH$_2$–C$H_3$, t, $J$ = 6.9 Hz), 1.32 (36H, HO–(CH$_2$)$_2$–(C$H_2$)$_6$–, m), 1.58 (8H, HO–CH$_2$–C$H_2$– and Ph–CH–C$H_2$–CH$_3$, m), 1.76 (8H, Ph–O–CH$_2$–C$H_2$–, m), 2.68 (2H, Ph–C$H$–, m), 2.87 (4H, Ph–C$H_2$–CH–, d, $J$ = 7.4 Hz), 3.64 (4H, HO–C$H_2$–, t, $J$ = 6.3 Hz), 3.92 (4H, monophenyl–O–C$H_2$–, t, $J$ = 6.3 Hz), 3.98 (4H, biphenyl–O–C$H_2$–, t, $J$ = 6.1 Hz), 6.81 (4H, ortho to ether of the monophenyl ring, d, $J$ = 8.5 Hz), 6.94 (4H, ortho to ether of the biphenyl ring, d, $J$ = 7.2 Hz), 7.04 (4H, ortho to methine of the monophenyl ring, d, $J$ = 7.7 Hz), 7.07 (4H, ortho to methylene of the biphenyl ring, d, $J$ = 7.3 Hz), 7.40 (4H, meta to methylene of the biphenyl ring, d, $J$ = 7.5 Hz), 7.48 (4H, meta to ether of the biphenyl ring, d, $J$ = 8.3 Hz).

**Synthesis of Dibromodecyl-TPB-10 Dimer (16).** **16** was prepared by the same procedure as that used for **11** except for the following conditions. Dimer **15** (0.421 g, 0.39 mmol) and CBr$_4$ (0.308 g, 0.93 mmol) were dissolved in 20 mL of dry THF. A solution of PPh$_3$ (0.244 g, 0.93 mmol) in dry THF (7 mL) was added dropwise to the reaction mixture and then it was stirred at room temperature overnight. After THF was evaporated, the resulting solid was dissolved in CHCl$_3$ and was precipitated in methanol and dried, and the precipite was purified by silica gel column chromatography. First, a mixture of hexanes and diethyl ether (2:1) was used as eluent to yield the pure and impure fractions. The impure fraction was further purified by silica gel column chromatography with a mixture of hexanes and diethyl ether (1:1) as eluent to yield the pure compound. The combined pure parts were dissolved in CHCl$_3$ and precipitated in methanol to yield a white solid (0.219 g, 46.6%). Purity (HPLC), >99%. $^1$H NMR (CDCl$_3$, TMS, $\delta$, ppm): 0.76 (6H, Ph–CH–CH$_2$–C$H_3$, t, $J$ = 7.6 Hz), 1.32 (40H, Br–(CH$_2$)$_2$–(C$H_2$)$_6$– and Ph–CH–C$H_2$–CH$_3$, m), 1.79 (10H, –O–CH$_2$–C$H_2$– and –C$H_2$–CH$_2$–Br, m), 2.68 (2H, Ph–C$H$–, m), 2.87 (4H, Ph–C$H_2$–CH–, d, $J$ = 7.4 Hz), 3.41 (4H, Br–C$H_2$–, t, $J$ = 6.8 Hz), 3.92 (4H, monophenyl–O–C$H_2$–, t, $J$ = 6.1 Hz), 3.98 (4H, biphenyl–O–C$H_2$–, t, $J$ = 6.2 Hz), 6.81 (4H, ortho to ether of the monophenyl ring, d, $J$ = 8.1 Hz), 6.94 (4H, ortho to ether of the biphenyl ring, d, $J$ = 7.9 Hz), 7.04 (4H, ortho to methine of the monophenyl ring, d, $J$ = 7.3 Hz), 7.07 (4H, ortho to methylene of the biphenyl ring, d, $J$ = 7.5 Hz), 7.40 (4H, meta to methylene of the biphenyl ring, d, $J$ = 7.6 Hz), 7.49 (4H, meta to ether of the biphenyl ring, d, $J$ = 8.4 Hz).

**Synthesis of Linear TPB-10 Tetramer (17).** The linear tetramer 17 was synthesized by the etherification of dibromodecyl-TPB-10 dimer (**16**) with monodecyl-TPB (**4a**, **4b**) using the same method as the one used for the synthesis of linear TPB-10 trimer (**12**). To a 25-mL single-neck flask equipped with a condenser and magnetic stirrer were added successively monodecyl-TPB (0.159 g, 0.347 mmol), 2.0 mL of 10 N NaOH aqueous solution (20 mmol), 2.0 mL of *o*-dichlorobenzene, dibromodecyl-TPB-10 dimer (0.200 g, 0.165 mmol), and TBAH (0.030 g, 0.087 mmol). A balloon filled with nitrogen was placed at the top of the condenser. The reaction mixture was stirred at 1100 rpm on a magnetic stirrer at 80 °C. After 30 min, the reaction mixture was diluted with water and chloroform, and the aqueous layer was removed. The organic layer was washed with water, followed by dilute hydrochloric acid, and 3 times with water. The product was precipitated in methanol. After it was dried under vacuum, the product was purified by silica gel column chromatography with a mixture of hexanes and CHCl$_3$ (1:1) as eluent. The solid was again precipitated in methanol from CHCl$_3$ solution to yield a white solid (0.192 g, 56.2%). Purity (HPLC), >99%. $^1$H NMR (CDCl$_3$, TMS, $\delta$, ppm): 0.76 (12H, Ph–CH–CH$_2$–C$H_3$, t, $J$ = 7.2 Hz), 0.88 (6H, –O–(CH$_2$)$_9$–C$H_3$, t, $J$ = 6.0 Hz), 1.27 and 1.33 (64H, CH$_3$–(C$H_2$)$_7$– and –O–CH$_2$–CH$_2$–(C$H_2$)$_6$–, m), 1.63 (8H, Ph–CH–C$H_2$–CH$_3$, m), 1.76 (16H, –O–CH$_2$–C$H_2$–, m), 2.68 (4H, Ph–C$H$–, m), 2.86 (8H, Ph–C$H_2$–CH–, d, $J$ = 6.7 Hz), 3.92 (8H, monophenyl–O–C$H_2$–, t, $J$ = 5.9 Hz), 3.97 (8H, biphenyl–O–C$H_2$–, t, $J$ = 6.2 Hz), 6.81 (8H, ortho to ether of the monophenyl ring, d, $J$ = 8.2 Hz), 6.94 (8H, ortho to ether of the biphenyl ring, d, $J$ = 8.1 Hz), 7.03 (8H, ortho to methine of the monophenyl ring, d, $J$ = 7.6 Hz), 7.07 (8H, ortho to methylene of the biphenyl ring, d, $J$ = 7.2 Hz), 7.39 (8H, meta to methylene of the biphenyl ring, d, $J$ = 7.1 Hz), 7.48 (8H, meta to ether of the biphenyl ring, d, $J$ = 9.5 Hz).

**Synthesis of Linear TPB-10 Polyethers for Fractionation.** Conventional liquid–liquid two phase (organic solvent–aqueous NaOH solution) phase-transfer-catalyzed polyetherification conditions were used for the preparation of TPB-10 polyethers. The polyetherifications were carried out under a nitrogen atmosphere at 80 °C in an *o*-dichlorobenzene–10 N NaOH water solution (10 times molar excess of NaOH versus phenol groups) in the presence of TBAH as phase-transfer catalyst.

**High Molecular Weight TPB-10.** To a 25-mL single-neck flask equipped with a condenser were successively added 0.325 g (1.02 mmol) of TPB (**1**), 2.0 mL of 10 N NaOH, 2.0 mL of *o*-dichlorobenzene, 0.300 g (1.00 mmol) of 1,10-dibromodecane (**5**), and 0.136 g (0.40 mmol, 20 mol % of phenol groups) TBAH. The reaction mixture was stirred at 1100 rpm on a magnetic stirrer at 80 °C under nitrogen. After 1 h, 1-bromodecane (**2**) was added to the reaction mixture so that polyethers containing only decyl chain ends are obtained. After 1 h, the organic and aqueous layers were diluted with chloroform and water, respectively, and the aqueous layer was separated. The organic layer was washed with water, followed by dilute aqueous HCl, and again 3 times with water. The polymer was separated by the precipitation of its solution into methanol to yield 0.436 g (93%)

of a white fibrous precipitate. The polymer was further purified by two additional precipitations from THF solution into water.

**Low Molecular Weight TPB-10.** The procedure was the same as that used for the high molecular weight TPB-10 except for the following conditions. TPB (0.319 g, 1.00 mmol) and 1,10-dibromodecane (0.276 g, 0.92 mmol) were polymerized in the presence of 1-bromodecane (0.0354 g, 0.16 mmol) for 30 min followed by the addition with 1-bromodecane (0.136 g, 0.40 mmol) to complete the alkylation of the terminal phenolates. The yield was 0.407 g (89%).

**Fractionation of TPB-10.** The high molecular weight TPB-10 (0.367 g) was dissolved in chloroform. Silica gel (12.6 g) was added to the chloroform solution and the solvent was evaporated. The polymer adsorbed on the silica gel was charged on the top of a column containing silica gel and was flushed 11 times with 100 mL of solvents. The solvents were mixtures of acetone and $CHCl_3$ whose ratios (acetone/$CHCl_3$) were 100/0, 90/10, 80/20, 70/30, 60/40, 50/50, 40/60, 30/70, 20/80, 10/90, and 0/100, and were charged in the order from 100/0 to 0.100. Each eluted fraction was collected and the solvents were evaporated on a rotary evaporator to produce the fractionated TPB-10 samples. Each fraction was dissolved in $CHCl_3$, filtered, precipitated in methanol, and dried under vacuum.

The procedure used for the low molecular weight TPB-10 was the same as that used for the high molecular weight TPB-10 except for the following conditions. The amount of polymer and silica gel were 0.230 and 26.0 g, respectively. The solvent ratios (acetone/$CHCl_3$) were 100/0, 90/10, 80/20, 70/30, 60/40, 55/45, 50/50, 45/55, 40/60, and 30/70 and were charged in the order from 100/0 to 30/70.

**Techniques.** 1-D $^1$H NMR (200 MHz) spectra were recorded on a Varian XL-200 NMR spectrometer. All spectra were acquired at room temperature with TMS as internal standard.

Relative molecular weights and purities were determined by gel permeation chromatography (GPC) and high-pressure liquid chromatography (HPLC). GPC analyses were carried out with a Perkin-Elmer series 10 LC equipped with an LC-100 column oven and a Nelson Analytical 900 series data station. The measurements were made by using a UV detector, chloroform as solvent (1 mL/min, 40 °C), two PL gel columns of $5 \times 10^2$ and $10^4$ Å, and a calibration plot constructed with polystyrene standards. HPLC analyses were performed with the same instrument with a PL gel column of $1 \times 10^2$ Å.

A Perkin-Elmer DSC-4 differential scanning calorimeter equipped with a TADS data station Model 3600 was used to determine thermal transitions. Heating and cooling rates were 20 °C/min in all cases. First-order transitions (crystalline–crystalline, crystalline–liquid crystalline, liquid crystalline–isotropic, etc.) were read at the maximum or minimum of the endothermic or exothermic peaks. Glass transition temperatures ($T_g$) were read at the middle of the change in the heat capacity. All heating and cooling scans after the first heating scan produced perfectly reproducible data. We will report the transitions collected from the first and second or subsequent heating scans and from the first cooling scan.

A Carl Zeiss optical polarizing microscope (magnification 100×) equipped with a Mettler FP 82 hot stage and a Mettler FP 800 central processor was used to observe thermal transitions and to analyze anisotropic textures.

## Results and Discussion

**Syntheses of TPB-10 Oligomers.** Schemes I to III outline the synthesis of linear TPB-10 monomer, dimer, trimer, and tetramer. All oligomers have decyl terminal groups at both chain ends so that the effect of terminal group on their phase behavior is excluded. The syntheses of monomer and dimer are straightforward. The etherification of TPB (**1**) with an equal molar amount of 1-bromodecane (**2**) yielded monomer TPB-10 (**3**), monodecyl TPB (**4a,4b**), and unreacted TPB (**1**). These compounds were separated by silica gel column chromatography as described in the experimental part. The reactivity of the phenolate group of the hydroxybiphenyl unit was higher than that of the hydroxyphenyl group according to the $^1$H NMR spectrum of the separated monodecyl TPB (**4a, 4b**). The ratio of **4b**/**4a** was 79/21.

The linear TPB-10 dimer was synthesized by the etherification of monodecyl-TPB (**4a, 4b**) with 1,10-dibromodecane (**5**). Therefore, due to the regiochemical structures indicated in Scheme I there are three possible constitutional isomers for this dimer. The most dominant structure is **6a**. The yield of this reaction step was not very high most probably due to the low solubility of the product resulting from the monoetherification of the dibromide with one monodecyl-TPB unit. This is an intermediate product of the dimer and precipitated out of solution during the reaction.

The linear TPB-10 trimer (Scheme II) and tetramer (Scheme III) were synthesized by following the same sequence of reactions, i.e., etherification of TPB and 1-bromo-9-decene, hydroboration of the double bonds followed by oxidation, bromination, and etherification with monodecyl-TPB except that, in the case of the tetramer, the etherification of monodecenyl-TPB was carried out with 1,10-dibromodecane to yield the didecenyl-TPB-10 dimer (**14**). In the synthesis of the tetramer, monodecenyl-TPB contained also a higher content of TPB alkylated at the phenolate group of the hydroxybiphenyl unit (**13b**). The exact ratio between **13a** and **13b** could not be calculated due to peaks overlapping. However, this ratio should not be far different from the ratio for the monodecyl-TPB (**4a, 4b**). The preferential alkylation to the hydroxybiphenyl group again leads to the preferential sequence of regiochemical structure of the trimer and tetramer. The hydroboration, bromination, and etherification reactions proceeded with high conversions. However, the yields of TPB-10 dimer **6** (38.1%), TPB-10 trimer **12** (64%), dihydroxydecyl-TPB-10 dimer **15** (69%), dibromodecyl-TPB-10 dimer **16** (47%), and TPB-10 tetramer **17** (56%) were relatively low. These low yields are due to the fact that minor impurities were severely overlapped with the desired products in the silica gel column and the products containing impurities were excluded to obtain the pure derivatives.

Due to the convenient solubility of TPB-10 oligomers and polymers, the synthetic procedures from Schemes I to III and variants of them can be extended to the preparation of monodisperse oligomers and polymers of TPB with any degree of polymerization.

**Characterization of TPB-10 Oligomers.** Table I summarizes the calculated and experimental molecular weights determined by GPC and the purities determined by HPLC for all linear TPB-10 oligomers. The purity of each oligomer was higher than 99%. The observed molecular weight was proportional to the degree of polymerization. The molecular weights obtained by GPC were consistently 1.60 times higher than the calculated ones. This indicates a larger hydrodynamic volume of TPB-10 in $CHCl_3$ compared to polystyrene standards which is most probably due to the presence of the rigid mesogenic unit. However, we will discuss their phase behavior by using the molecular weights obtained by GPC.

Thermal transition temperatures and the corresponding enthalpy changes of TPB-10 oligomers determined by DSC are summarized in Table I. All TPB-10 oligomers exhibit only melting transitions during first heating scans. The dimer, trimer, and tetramer exhibit isotropic–nematic monotropic transitions, i.e., only during cooling scans. Their mesophase was identified by optical polarized microscopy. All three oligomers exhibit a typical schlieren nematic texture. Figure 1 presents a representative texture of the nematic phase displayed by these oligomers. The particular texture from Figure 1 is for the tetramer. The monomer exhibits several exothermic peaks during the

Table I. Characterization of Linear TPB-10 Oligomers

| oligomer | $M_n \times 10^3$ (calculated) | $M_n \times 10^3$ (determined) | purity (%) | thermal transitions (°C) and corresponding enthalpy changes (kcal/mru) in parentheses[a] heating | cooling |
|---|---|---|---|---|---|
| monomer | 0.599 | 0.96 | >99 | k 57.5 (12.01) i<br>k 45.8 (−0.37) k 58.9 (11.06) i | i 23.0 × 18.8 × 12.3 (8.57[b]) i |
| dimer[c] | 1.056 | 1.67 | >99 | g 47.3 k 52.4 k 67.5 k 81.8 k 98.0 (7.75[b]) i<br>k 8.0 k 31.2 (−3.16[b]) 69.3 k 94.4 (6.85)[b] i | i 57.6 (1.65) n 26.3 (1.23) k −0.4 (0.37) k |
| trimer | 1.512 | 2.42 | >99 | K 84.2 k 88.3 (6.17[b]) i<br>g 9.5 n 77.9 (2.31) i | i 70.0 (2.25) n 2.4 g |
| tetramer | 1.969 | 3.07 | >99 | k 76.8 k 84.5 k 90.0 (5.19[b]) i<br>g 14.8 n 84.9 (2.35) i | i 77.8 (2.31) n 8.8 g |

[a] Data on the first line are from first heating and cooling scans. Data on the second line are from second heating scan. [b] Overlapped peaks. [c] The nematic–isotropic transition (63 °C) on heating was observed when it was heated right after the isotropic–nematic transition on cooling.

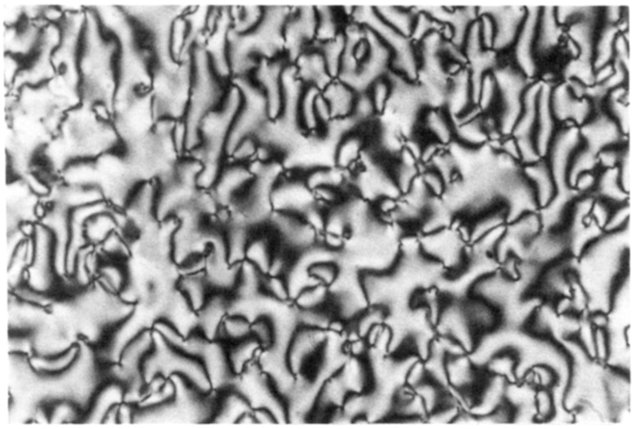

**Figure 1.** Typical optical polarized micrograph of the texture (×100) exhibited by the nematic phase of linear TPB-10 tetramer annealed at 71.2 °C for 4 min.

cooling scan. However, these phases could not be identified since the crystallization occurred very fast during annealing on the optical microscope. The trimer and the tetramer did not crystallize during both cooling and second or subsequent heating scans. In the case of the dimer, the nematic–isotropic transition could be observed also on the heating scan by reheating right after the isotropic–nematic transition from the cooling scan. Both the nematic–isotropic and the isotropic–nematic transition temperatures ($T_{ni}$ and $T_{in}$) increase with increasing the molecular weight of the oligomer. Simultaneously, the crystallization tendency of these oligomers decreases with increasing their molecular weight.

Table II summarizes the purities, the thermal transition temperatures, and the corresponding enthalpy changes of all the intermediate compounds used to synthesize the linear TPB-10 oligomers. It is interesting to see how the functional group of the terminal alkyl tail influences the phase behavior of these oligomers. This can be done by inspecting the DSC thermograms of these intermediary compounds. All monomers with various chain ends show one melting peak during their first heating scan. The melting temperature decreases depending on the terminal groups in the following order: monodecenyl-TPB (**13, 13b**) = monodecyl-TPB (**4a, 4b**) > dihydroxydecyl-TPB-10 monomer (**10**) > TPB-10 monomer (**3**) = dibromodecyl-TPB-10 monomer (**11**) > didecenyl-TPB-10 monomer (**9**). The same trend was observed during their second heating scan. During cooling scan, a nematic mesophase was observed for all monomers except for the didecenyl-TPB-10 (**9**) monomer and TPB-10 monomer (**3**). TPB-10 monomer shows a small shoulder and two peaks. However, as mentioned above it is not yet known if these peaks correspond to mesomorphic transitions. Dihydroxydecyl-TPB-10 monomer (**10**) exhibits a higher isotropic–nematic transition temperature (60 °C) and associated enthalpy change than those of the other oligomers. This may be explained by the stabilization of its mesophase via hydrogen bonding. Although phenol groups which also generate hydrogen bonding exist in the monodecenyl- and monodecyl-TPB (**13a** and **13b**, **4a** and **4b**), these compounds exhibit lower $T_{in}$ which are almost identical to those of dibromodecyl-TPB-10 monomer (**11**). The lack of one alkyl group in these compounds may decrease the stability of their mesophase. It is interesting that monodecenyl-TPB (**13a, 13b**) shows a lower $T_{ni}$ and associated enthalpy change compared to monodecyl-TPB (**4a, 4b**) since the only difference is the presence of the vinyl group in the former one.

All dimers with various terminal groups display a monotropic nematic mesophase. During first heating

Table II. Characterization of Linear TPB-10 Oligomers with Various Terminal Groups

| oligomers | purity (%) | thermal transitions (°C) and corresponding enthalpy changes (kcal/mru) in parentheses[a] heating | cooling |
|---|---|---|---|
| monodecyl-TPB | >99 | k 82 (11.2) i<br>g 5 n 18 (0.58) i 20 (−3.11) k 42 (−3.88) k 75 k 80 (9.32[b]) i | i 12 (1.48) n −5 g |
| monodecenyl-TPB | >99 | k 83 (9.33) i<br>g 8 n 4 (1.06) i 11 k 19 k 38 (6.54[b]) k 80 k 85 (9.06) i | i −1 (0.67) n −11 g |
| didecenyl-TPB-10 monomer | 96.0 | k 49 (9.82) i<br>k 31 k 38 (6.43[b]) i | i 10 (5.86) k |
| dihydroxydecyl-TPB-10 monomer | 97.7 | k 70 (11.8) k 84 (0.34) i<br>k 52 k 58 k 65 (−3.01[b]) k 85 (6.35) i | i 60 (2.06) n 35 (2.32) k |
| dibromodecyl-TPB-10 monomer | 97.3 | k 57 (9.69) i<br>k 13 k 31 (3.04b) k 54 (8.27) i | i 13 (0.65) n −16 k |
| didecenyl-TPB-10 dimer | >99 | k 52 k 69 k 81 k 90 (8.53[b]) i<br>g −9 n 8 (−4.10) k 60 k 89 (5.86[b]) i | i 50 (1.25) n 18 (0.15) k 6.2 g |
| dihydroxydecyl-TPB-10 dimer | >99 | k 54 k 92 (7.38[b]) i<br>k 62 (0.79) k 81 k 90 (5.75[b]) i | i 68 (2.48) n 48 (1.90) k |
| dibromodecyl-TPB-10 dimer | >99 | k 83 k 98 k 113 (8.00[b]) k<br>k 16 (0.46) k 82 k 112 (8.68[b]) i | i 51 (1.13) n 35 (3.59) k |

[a] Data on the first line are from first heating and cooling scans. Data on the second line are from second heating scan. [b] Overlapped peaks.

**Scheme IV. Preparation of High Molecular Weight TPB-10 Polyether with Terminal Decyl Groups**

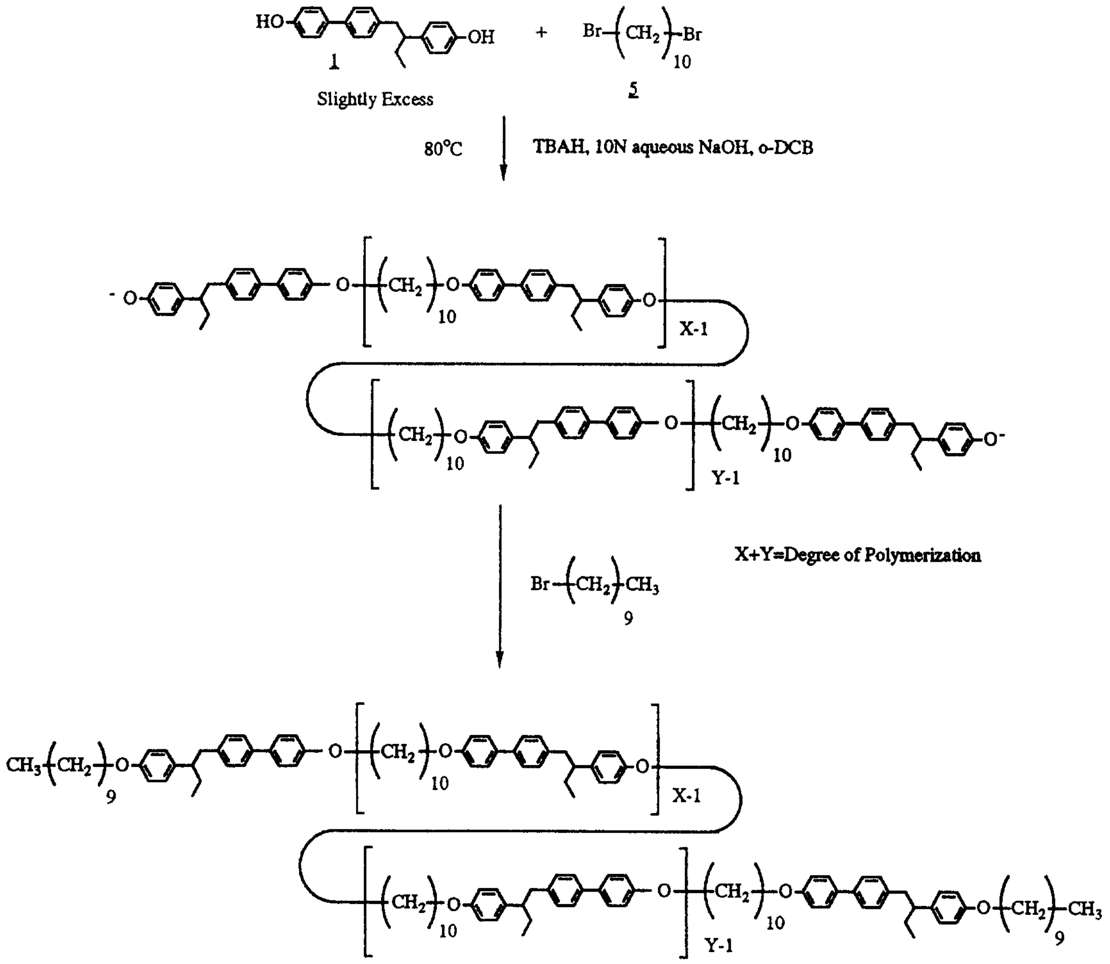

**Scheme V. Preparation of Low Molecular Weight TPB-10 Polyether with Terminal Decyl Groups**

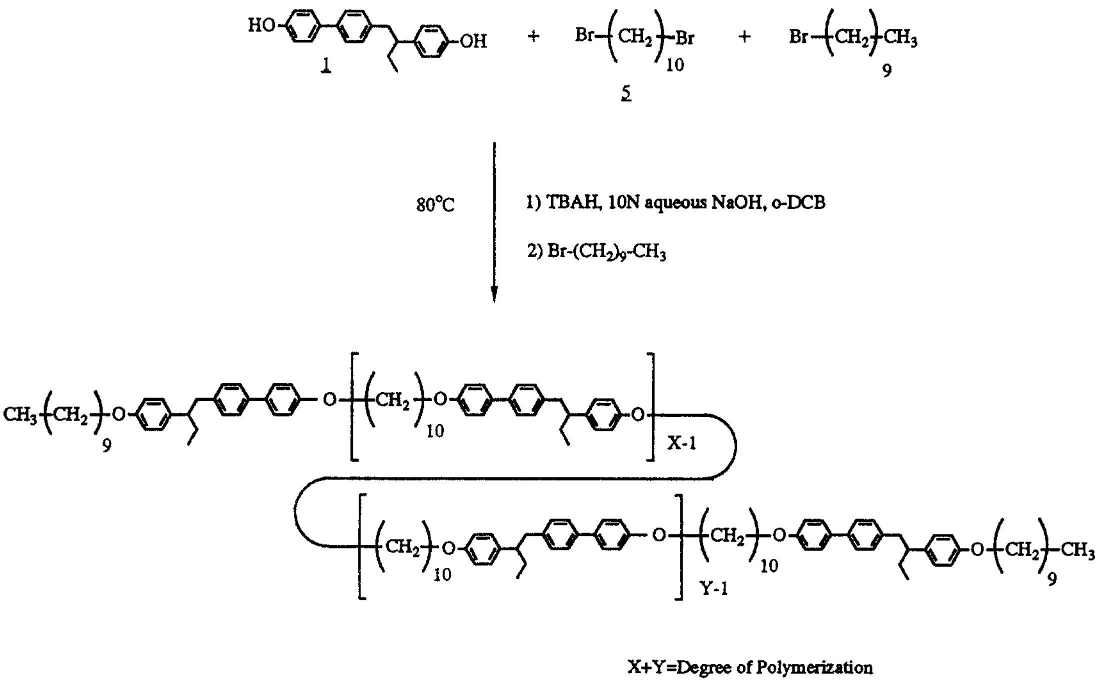

scans, all dimers exhibit rather broad melting peaks. The order of their melting temperature is as follows: dibromodecyl-TPB-10 dimer (16) > didecyl-TPB-10 dimer (6) > dihydroxydecyl-TPB-10 dimer (15) = didecenyl-TPB-10 dimer (14). This order is different from that exhibited by the monomers. During cooling scans, in all cases, both isotropic–nematic and nematic–crystalline transitions were observed. The order of $T_{\text{in}}$ is as follows: dihydroxydecyl-TPB-10 dimer (11) > didecyl-TPB-10 dimer (6) > dibromodecyl-TPB-10 dimer = didecenyl-TPB-10 dimer. This order is opposite to that observed for the melting temperature except for the case of didecenyl-TPB-10 dimer and is similar to the order of $T_{\text{in}}$ found for TPB monomers. Again, hydrogen bonding must be responsible for the higher transition temperature of dihydroxydecyl-TPB-10 dimer.

Table III. Characterization of Fractionated Polyethers from High Molecular Weight TPB-10

| solvents (CHCl$_3$/acetone) | yield (%) | $M_n \times 10^4$ | $M_n/M_w$ | thermal transitions (°C) and corresponding enthalpy changes (kcal/mru) in parentheses[a] heating | cooling |
|---|---|---|---|---|---|
| original | | 1.33 | 3.54 | g 38.3 n 111.3 (2.76) i<br>g 38.1 n 111.6 (2.75) i | i 95.6 (2.70) n 30.6 g |
| 0/100 | 4.2 | 0.16 | 2.63 | | |
| 20/80 | 2.1 | 0.555 | 1.16 | g 26.9 n 96.4 (2.24) i<br>g 27.0 n 97.5 (2.37) i | i 89.9 (2.37) n 20.9 g |
| 40/60 | 4.6 | 1.13 | 1.18 | g 36.5 k 41.2 (0.16) n 103.5 (2.64) i<br>g 32.6 n 103.8 (2.69) i | i 95.3 (2.68) n 26.6 g |
| 50/50 | 13.5 | 2.09 | 1.20 | g 38.1 k 44.7 (0.10) k 60.0 (0.08) n 108.0 (2.78) i<br>g 37.0 n 108.2 (2.83) i | i 98.0 (2.79) n 30.5 g |
| 60/40 | 23.2 | 3.58 | 1.28 | g 39.0 n 44.9 (–0.04) n 112.2 (2.86) i<br>g 40.9 n 112.6 (2.85) i | i 98.4 (2.81) n 33.3 g |
| 70/30 | 20.2 | 5.63 | 1.34 | g 42.2 n 67.8 (–0.27) n 114.0 (2.82) i<br>g 42.3 n 114.0 (2.84) i | i 98.1 (2.88) n 35.3 g |
| 80/20 | 9.8 | 5.72 | 1.47 | g 47.5 n 52.8 n 67.6 (–0.76[b]) n 114.4 (2.82) i<br>g 44.1 n 114.4 (2.88) i | i 97.8 (2.81) n 35.9 g |
| 90/10 | 1.0 | 5.49 | 1.48 | | |
| 100/0 | 0.4 | 5.73 | 1.44 | | |

[a] Data on the first line are from first heating and cooling scans. Data on the second line are from second heating scan. [b] Overlapped peaks.

Table IV. Characterization of Fractionated Polyethers from Low Molecular Weight TPB-10

| solvents (CHCl$_3$/acetone) | yield (%) | $M_n \times 10^4$ | $M_n/M_w$ | thermal transitions (°C) and corresponding enthalpy changes (kcal/mru) in parentheses heating | cooling |
|---|---|---|---|---|---|
| original | | 0.59 | 2.43 | g 46.7 k 50.0 k 56.6 (1.56) n 100.6(2.49) i<br>g 25.7 n 99.7 (2.63) i | i 91.8 (2.47) n 21.7 g |
| 0/100 | 19.9 | 0.30 | 1.40 | | |
| 10/90 | 2.1 | 0.52 | 1.16 | g 26.5 k 44.1(0.40) n 95.1 (2.40) i<br>g 26.6 n 95.6 (2.39) i | i 88.6 (2.39) n 19.8 g |
| 20/80 | 4.0 | 0.66 | 1.16 | g 24.7 k 60.8 k 70.8 n 95.3 (6.74[b]) i<br>g 28.3 n 99.2 (2.54) i | i 89.9 (2.46) n 21.1 g |
| 30/70 | 5.5 | 0.82 | 1.18 | g 32.6 k 36.3 (0.12) n 101.0 (2.51) i<br>g 31.3 n 101.5 (2.64) i | i 93.5 (2.54) n 24.4 g |
| 40/60 | 7.8 | 1.01 | 1.28 | g 37.8 k 41.7 (0.21) n 105.4 (2.65) i<br>g 35.0 n 105.1 (2.66) i | i 95.5 (2.56) n 28.7 g |
| 45/55 | 7.9 | 1.43 | 1.21 | g 40.6 k 43.9 (0.21) n 106.0 (2.74) i<br>g 35.8 n 105.9 (2.81) i | i 96.9 (2.69) n 29.7 g |
| 50/50 | 8.0 | 1.18 | 1.56 | | |
| 55/45 | 17.3 | 1.13 | 1.50 | | |
| 60/40 | 4.4 | 1.25 | 1.75 | | |
| 70/30 | 5.1 | 1.85 | 1.49 | | |

[a] Data on the first line are from first heating and cooling scans. Data on the second line are from second heating scan. [b] Overlapped peaks.

The results mentioned above demonstrate clearly that the terminal groups affect the phase behavior of linear oligomers. The contribution of terminal groups decreases with the increase of the degree of oligomerization. Therefore, it is very important to maintain the terminal groups consistent through the entire range of molecular weights in order to extract only the effect of molecular weight on phase transitions.

**Fractionation of TPB-10 Polyethers.** Schemes IV and V present the polymerization reaction used in the synthesis of high molecular weight TPB-10 and of low molecular weight TPB-10, respectively. The polyether with high molecular weight was synthesized to produce via fractionation high molecular weight fractions of TPB-10. This polymerization was carried out with a slight excess of TPB (2 mol %) so that most of polymer chain ends remain as phenolate anions at the end of polymerization. Following the polymerization, the phenolate chain ends were end capped with 1-bromodecane in situ. The low molecular weight TPB-10 was synthesized by replacing the 8 mol % of the dibromide for 16 mol % of 1-bromodecane. The polymerization was terminated by the addition of 1-bromodecane to make sure that no unreacted phenol chain ends existed. The number average molecular weights ($M_n$) and polydispersities ($M_w/M_n$) of the resulting TPB-10 polyethers were 1.33 × $10^4$ and 3.54 and 0.59 × $10^4$ and 2.43, respectively. Both polydispersities are significantly higher than the values expected from the most probable distribution. This is due to the formation of cyclic oligomers during polymerization, which cannot propagate further and widens the polydispersity leading to a sample containing two polymer homologous series.[11]

The fractionation of these polymers was carried out by a conventional column method with chloroform as solvent and acetone as nonsolvent.[16] Tables III and IV summarize the yields, number average molecular weights, polydispersities, phase transition temperatures, and the corresponding enthalpy changes of the fractionated polyethers from the high and respectively low molecular weights TPB-10, as well as of the original polyethers before fractionation. Table III summarizes the fractionation results of TPB-10 with high molecular weight. The molecular weight of fractionated polymers increases with increasing the content of CHCl$_3$ up to 70% of the acetone fraction which most probably contains only cyclic oligomers. The maximum yield separated for each fraction is obtained at about a 60% CHCl$_3$ content and becomes significantly lower above 70% CHCl$_3$ content since there was only little polymer remaining in the column. The total yield of the recovered polymer was 79.0%.

On the other hand, the fractionation of the low molecular weight TPB-10 was not as successful as that of the high molecular weight TPB-10. A very good fractionation occurred up to 45% CHCl$_3$ content in the solvent mixture.

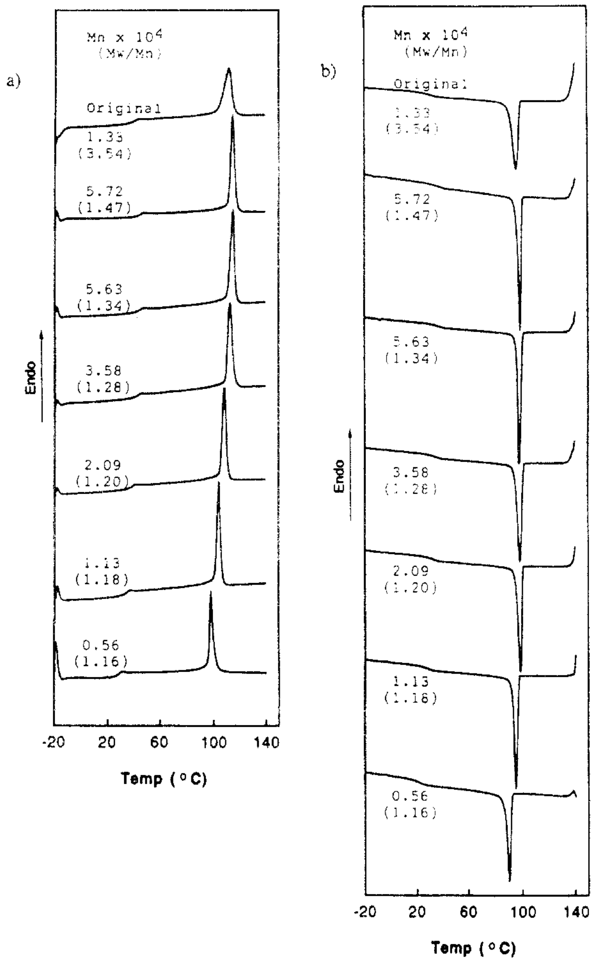

**Figure 2.** DSC thermograms of the second heating (a) and cooling scans (b) of the fractionated polyethers separated from the high molecular weight TPB-10 and of the original high molecular weight TPB-10 before fractionation.

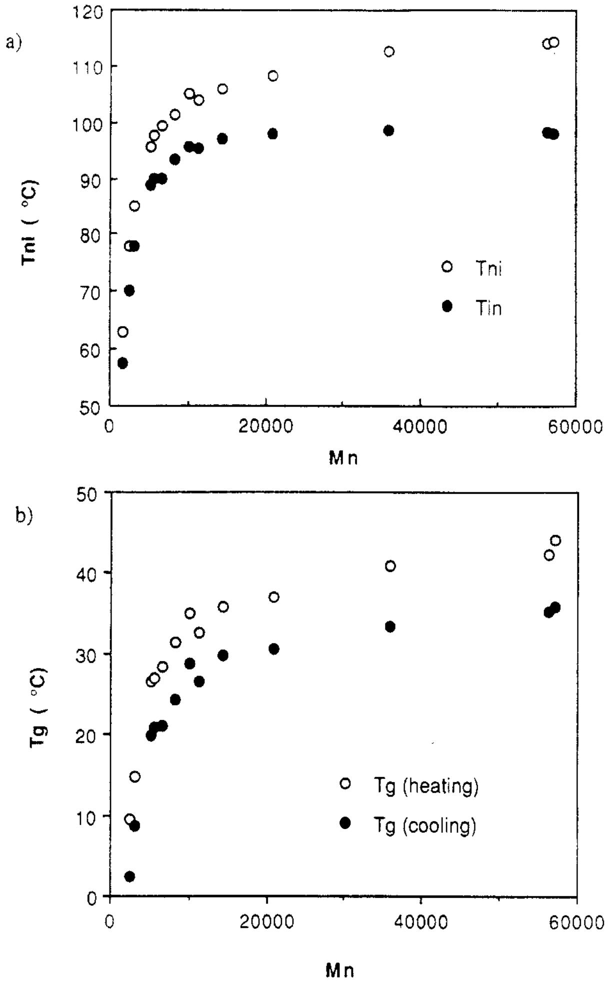

**Figure 3.** Nematic-isotropic transition temperatures ($T_{ni}$, ○; $T_{in}$, ●) (a) and glass transition temperatures ($T_g$, ○, second heating scan; ●, cooling scan) (b) of the fractional linear TPB-10 polyethers and of the oligomers plotted versus number average molecular weight ($M_n$).

The molecular weights of polymers fractionated with the solvents containing 20% and 40% of $CHCl_3$ were almost the same as those of the polymers fractionated with the same solvents from the high molecular weight TPB-10 sample. However, the fraction separated with 50% $CHCl_3$ showed a bimodal molecular weight distribution. The polydispersity remained relatively high (>1.5) above 50% $CHCl_3$ in the mixture. This is due to the fact that crystallization of the charged polymer took place during the evaporation of solvent and prevented the fractionation since the low molecular weight TPB-10s crystallize easier than the high molecular weight ones, especially from solution. The polyethers with narrow polydispersity obtained by fractionation were used to evaluate the effect of molecular weight on phase transitions.

**Phase Transitions of TPB-10 Polymers.** Figure 2 presents as an example the DSC thermograms of the second heating and cooling scans of polymers obtained from the fractionation of the high molecular weight TPB-10 sample and of the original high molecular weight TPB-10 before the fractionation. All the DSC results including those of the first heating scans and of the samples obtained by the fractionation of the low molecular weight TPB-10 are summarized in Tables III and IV. The fractionated polyethers with molecular weights lower than 40 000 show a small melting transition on their first heating scan (Tables III and IV) and an enantiotropic nematic mesophase. Since the tetramer, trimer, and dimer exhibit a monotropic nematic phase, the monotropic phase is transformed into an enantiotropic phase by increasing the molecular weight of TPB-10. This behavior was predicted theoretically[1b-d] and also was observed for the case of both main chain[3-7] and side chain liquid crystalline polymers.[2] As seen in Figure 2, on cooling and second heating scans, only glass and nematic–isotropic transitions were observed. All fractionated polyethers with narrow polydispersities exhibit very sharp nematic–isotropic transition peaks regardless of molecular weight. The width of these transition peaks is not affected, within the range reported here, by their polydispersity. On the other hand, the original TPB-10 before fractionation exhibits only a slightly broader transition peak (Figure 2). In Figure 3, $T_{ni}$, $T_{in}$, and $T_g$ values obtained from heating and cooling scans were plotted versus the number average molecular weight ($M_n$) obtained by GPC. Both $T_{ni}$ and $T_{in}$ increase abruptly with increasing their number average molecular weight up to about 15 000 to 20 000. Above this molecular weight value, $T_{ni}$ continues to increase with a much lower slope while $T_{in}$ stays constant or even decreases to a very small extent at very high molecular weights (Figure 3a). $T_g$ follows a similar trend (Figure 3b). $T_{ni}$, $T_{in}$, and $T_g$ (heating) and $T_g$ (cooling) were plotted versus reciprocal $M_n$ in Figure 4. Linear relationships of $T_{ni}$, $T_{in}$, $T_g$ (heating), and $T_g$ (cooling) versus $1/M_n$ were obtained except for the region at high molecular weight. For the glass transition, this relation can be expected from the Fox–Flory equation which is based on the free-volume theory.[17] A detailed inspection of Figure 4 leads to the following interesting observation. In Figure 4a, $T_{ni}$ deviates from the linear dependence of $1/M_n$ toward the upper side above $M_n$ = 20 000, while $T_{in}$ deviates toward

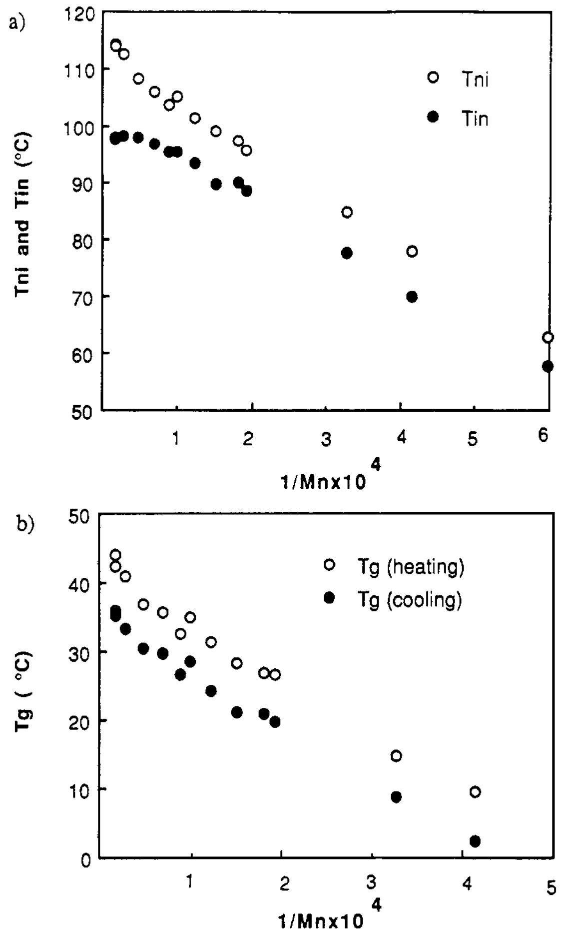

**Figure 4.** Nematic–isotropic transition temperatures ($T_{ni}$, ○; $T_{in}$, ●) (a) and glass transition temperatures ($T_g$, ○, second heating scan; ●, cooling scan) (b) of the fractionated linear TPB-10 polyethers and of the oligomers plotted versus reciprocal number average molecular weight ($1/M_n$).

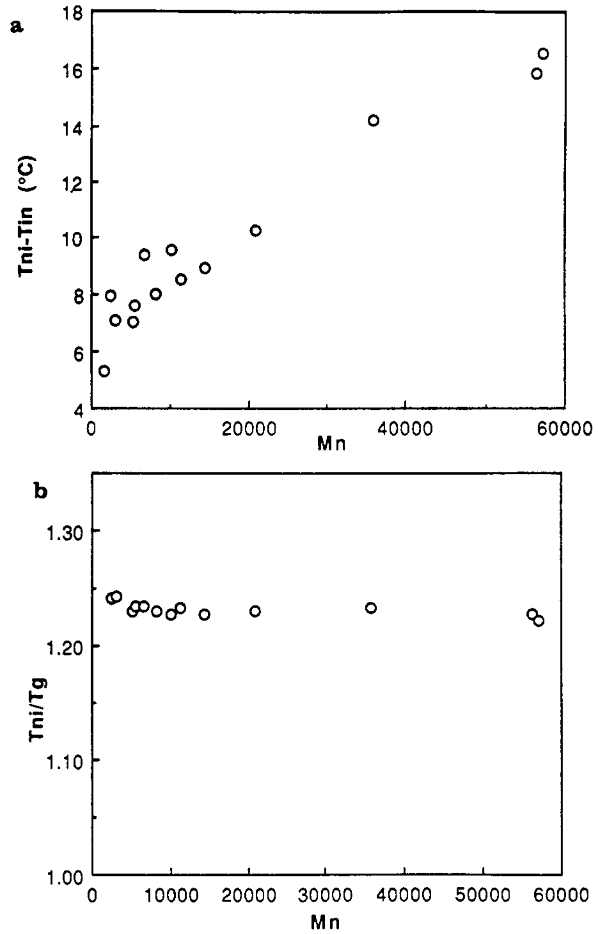

**Figure 5.** (a) Supercooling of the isotropization transition ($T_{ni} - T_{in}$, in °C) of TPB-10 plotted versus number average molecular weight ($M_n$). (b) Ratio $T_{ni}/T_g$ of TPB-10 plotted versus number average molecular weight ($M_n$). (Data from second heating scan.)

the lower side above $M_n$ = 20 000. This phenomenon can be explained by supercooling and superheating effects due to the high viscosity of the system in the high molecular weight region. The supercooling ($T_{ni} - T_{in}$, in °C) was plotted versus $M_n$ in Figure 5a. Actually, it increases linearly with increasing the molecular weight. Therefore, at low molecular weights the isotropization transition is thermodynamically controlled while at high molecular weights (i.e., $M_n$ higher than 20 000), by analogy with other first-order transitions in polymers, it becomes kinetically controlled. The kinetic effect on the isotropization temperature of the nematic mesophase is, as expected, much lower than on crystalline phases. On the other hand, both $T_g$ values obtained from cooling and heating scans deviate from the linear relations toward the upper side (Figure 4b). Another interesting observation is that the ratio $T_{ni}/T_g$ remains almost constant throughout the entire range of molecular weights as indicated in Figure 5b. Although glass transition is a second-order phase transition while nematic–isotropic is a first order one, there are surprising similarities between them in terms of their dependence on molecular weight at least for the case of this particular polymer.

Although all these polyethers exhibit typical schlieren nematic textures, there is a dependence of the rate of evolution of the texture on molecular weight. Namely, the evolution rate increases significantly with decreasing molecular weight. Figure 6 presents two representative examples. The texture (Figure 6b) exhibited by the high molecular weight sample ($M_n = 3.58 \times 10^4$) is much smaller than that (Figure 6a) of the low molecular weight sample ($M_n = 1.13 \times 10^4$) at the same evolution time although the former was annealed at a higher temperature. Regardless of their polydispersity, TPB-10 linear polymers do not exhibit a biphasic morphology at their isotropization transition.

In Figure 7, the enthalpy changes ($\Delta H$) associated with the nematic–isotropic and isotropic–nematic transitions were plotted versus $M_n$ and $1/M_n$, respectively. Again, $\Delta H$ increases with increasing molecular weight and levels off above a number average molecular weight of about 20 000. $\Delta H$ also shows a linear relationship versus $1/M_n$ up to $1/M_n = 2 \times 10^{-4}$. However, $\Delta H$ deviates toward the upper side below the tetramer region. This trend may be due to the fact that $\Delta H$ was calculated based on the molecular weight of the repeat unit. However, the contribution from chain ends to $\Delta H$ is not negligible for low molecular weight oligomers such as trimer and tetramer.

**Comparison of the Phase Transitions of Linear and Macrocyclic TPB-10 Oligomers and Polymers.** In some previous publications from this series we have predicted and demonstrated that macrocyclic derivatives based on TPB and $\alpha,\omega$-dibromoalkanes should display at a certain ring size a higher ability to generate liquid crystalline phases than the corresponding linear low and high molecular weight homologous.[11] This is due to the fact that at a certain ring size a suitable combination between ring size, spacer, and TPB lengths, the contribution of ring strain, molecular architecture, and absence of chain ends makes the cyclic molecules more rigid than their linear counterpart.

The results on linear oligomers provided by this paper allow for the the first time a quantitative comparison

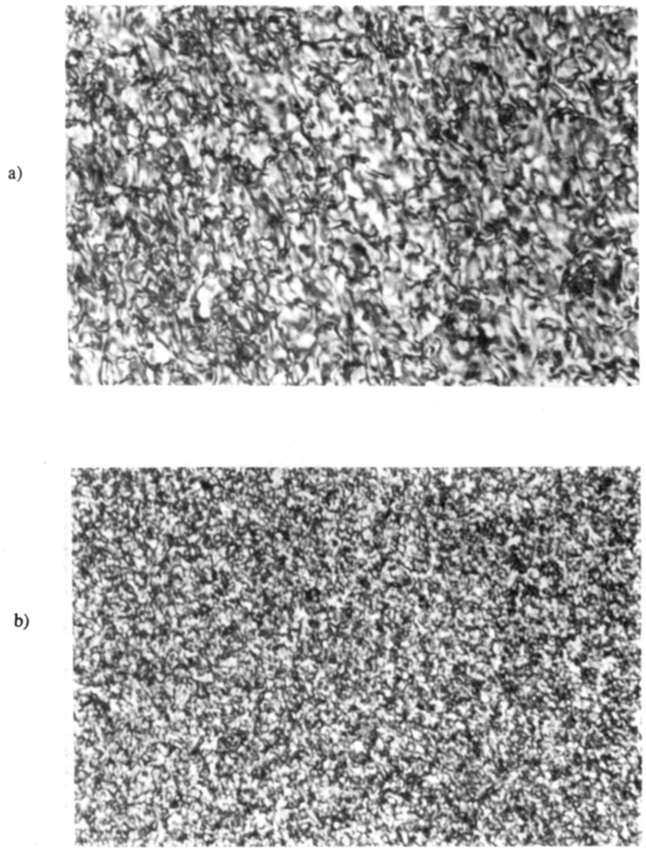

**Figure 6.** Typical optical polarized micrographs (×100) of the representative texture exhibited by the nematic phase of the linear TPB-10 polyethers: (a) $M_n = 1.13 \times 10^4$, annealed at 84.2 °C for 22 min; (b) $M_n = 3.58 \times 10^4$, annealed at 95.4 °C for 22 min.

between the phase behavior of linear and macrocyclic liquid crystals of TPB-10 to be made. The macrocyclic monomer [TPB-(c)10(1)] to pentamer [TPB-(c)10(5)] and a high molecular weight macrocyclic of $M_n$ = 11 800 which contains about 40% linear polymer were reported previously.[11a]

Figure 8 presents the plot of the isotropic–nematic ($T_{in}$) transition temperatures of linear and macrocyclic oligoethers and polymers as a function of their degree of polymerization (DP). A brief inspection of the calculated and experimentally determined $M_n$ (by GPC) of linear oligomers (Table I) shows that the experimental values are consistently larger by a factor of 1.60. Therefore, this factor was used to make corrections in the values of experimental $M_n$ data of TPB-10 from Tables III and IV which were used to calculate their degrees of polymerization from Figure 8. The corresponding correction factor for cyclics is 1.3.[11a] Consequently, the DP data from Figure 8 are absolute values. The macrocyclic and linear monomers are liquid and crystalline, respectively. Larger linear oligomers display a monotropic nematic mesophase, while larger macrocyclics display monotropic (dimer and trimer) and enantiotropic (tetraner and pentamer) nematic mesophases. Therefore, we will discuss only their $T_{in}$ transition. The macrocyclic dimer has a $T_{in}$ that is 16 °C lower than that of its corresponding linear dimer. However, the cyclic trimer and tetramer have $T_{in}$ values which are 17 and 46 °C higher, respectively, than of their linear homologues. The linear pentamer is not available while the cyclic pentamer is. The trend of the plot in Figure 8 shows that the pentamer still displays a much higher isotropization temperature than that expected for the linear structure. However, the transition temperature of the cyclic pentamer is lower than that of the cyclic tetramer.

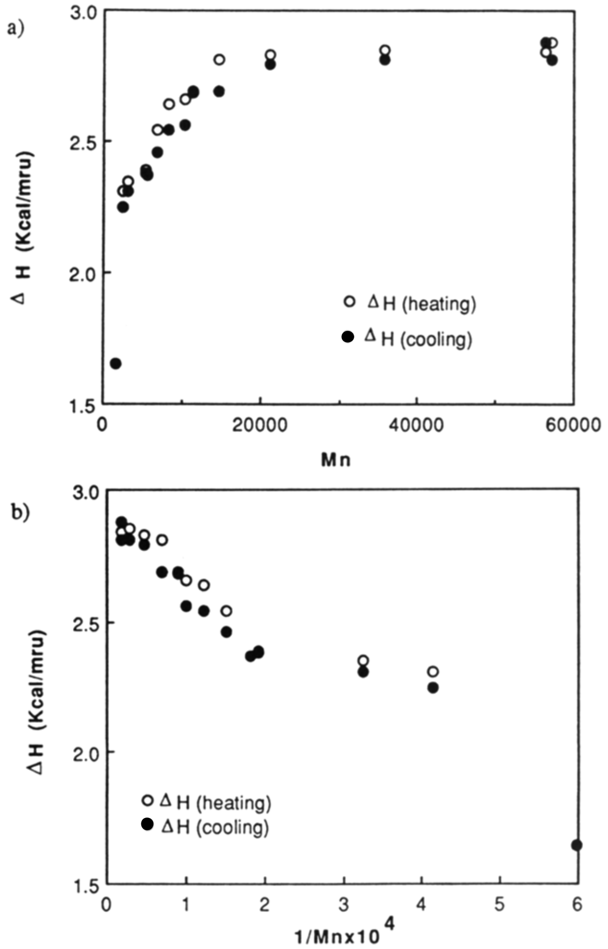

**Figure 7.** Enthalpy change (Δ*H*) associated with the nematic–isotropic (○, second heating scan) and isotropic–nematic (●, cooling scan) transitions of TPB-10 plotted versus number average molecular weight ($M_n$) (a) and 1/*Mn* (b).

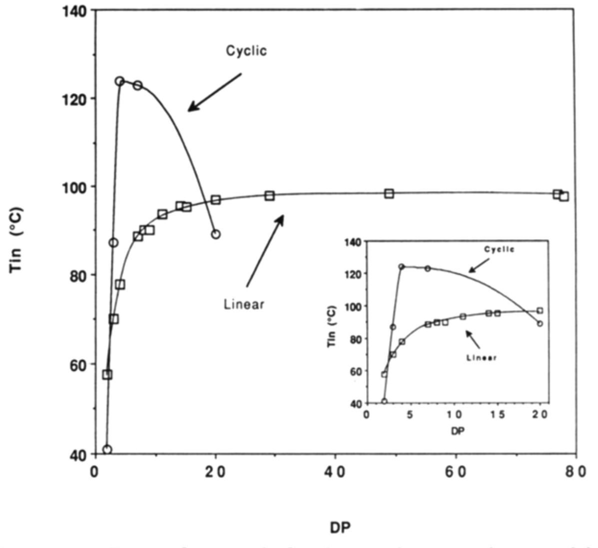

**Figure 8.** Dependence of the isotropic–nematic transition temperatures ($T_{in}$) of linear (□) and macrocyclic (○) TPB-10 on their degree of polymerization (DP). Transition temperatures of macrocyclics are from ref 11a.

This should be due to the release of ring strain which takes place on going from tetramer to pentamer. The high molecular weight cyclic structure has a broad polydispersity ($M_n/M_w$ = 1.53) and displays a lower transition temperature than that of its linear structure.

Theoretically, if the high molecular weight cyclic structure would be pure and monodispersed, it would have to exhibit an identical transition with the linear structure.

Nevertheless, the trend from Figure 8 demonstrates that our predictions were correct.[11]

Few other differences between linear and cyclic oligomers are as follows. The enthalpy changes associated with the isotropization transition of the macrocyclic dimer is 20 times lower than that of the linear dimer. The corresponding value of the cyclic trimer is 7 times lower while those of the cyclic tetramer and pentamer are only 2 times lower than those of the linear homologues (Table I and ref 11a). The glass transition temperatures of the linear trimer and tetramer are about 17 °C lower than those of the corresponding macrocyclics. At the same time, the crystallization tendency of the macrocyclics is much lower than that of the linear homologues. For example certain macrocyclics crystallize quite easy from solution but only with difficulty or not at all from the melt phase.

The miscibility of macrocyclics with their corresponding linear polymers is an additional problem of interest which is under investigation. Both optical polarized microscopy and NMR spectroscopy have shown the absence of a biphase in both fractionated and unfractionated samples of linear TPB-10 polymers.

We believe that the implications of these effects of the high molecular weight on phase transitions, particularly of its influence on the degree of supercooling of the isotropization transition, should be considered very carefully when trying to make quantitative statements about the influence of molecular architecture on the phase behavior of liquid crystalline polymers.

**Acknowledgment.** Financial support by the National Science Foundation, Polymers Program (DMR-92-06781), is gratefully acknowledged.

## References and Notes

(1) (a) This is Part 32 in the Series Liquid Crystalline Polyethers Based on Conformational Isomerism; for part 31 in this series see ref 10. (b) Percec, V.; Keller, A. *Macromolecules* **1990**, *23*, 4347. (c) Keller, A.; Ungar, G.; Percec, V. In *Liquid Crystalline Polymers*; Weiss, R. A., Ober, C. K., Eds.; ACS Symposium Series 435, American Chemical Society: Washington, DC, 1990; p 308. (d) Percec, V.; Tomazos, D. In *Comprehensive Polymer Science, First Supplement*; Allen, G., Ed., Pergamon Press: Oxford, 1992; pp 300–383.

(2) (a) Percec, V.; Pugh, C. In *Side Chain Liquid Crystal Polymers*; McArdle, C. B., Ed.; Blackie and Son Ltd.: Glasgow, and Chapman and Hall: New York, 1989; p 30. (b) Percec, V.; Hahn, B. *Macromolecules* **1989**, *22*, 1588. (c) Stevens, H.; Rehage, G.; Finkelmann, H. *Macromolecules* **1984**, *17*, 851. (d) Percec, V.; Tomazos, D.; Pugh, C. *Macromolecules* **1989**, *22*, 2259. (e) For a review on molecular engineering of side chain liquid crystalline polymers by living cationic polymerization see: Percec, V.; Tomazos, D. *Adv. Mater.* **1992**, *4*, 548. (f) Komiya, Z.; Pugh, C.; Schrock, R. R. *Macromolecules* **1992**, *25*, 3609, 6586, 6593.

(3) (a) Kumar, R. S.; Clough, S. B.; Blumstein, A. *Mol. Cryst. Liq. Cryst.* **1988**, *157*, 387. (b) Blumstein, R. B.; Blumstein, A. *Mol. Cryst. Liq. Cryst.* **1988**, *165*, 361, and references cited therein.

(4) Majnusz, J.; Catala, J. M.; Lenz, R. W. *Eur. Polym. J.* **1983**, *19*, 1043.

(5) Zhou, Q. F.; Duan, X. Q.; Liu, X. Q. *Macromolecules* **1986**, *19*, 247.

(6) (a) Percec, V.; Nava, H. *J. Polym. Sci., Polym. Chem. Ed.* **1987**, *25*, 405 and 1943. (b) Feijoo, J. L.; Ungar, G.; Owen, A. J.; Keller, A.; Percec, V. *Mol. Cryst. Liq. Cryst.* **1988**, *155*, 487.

(7) Laus, M.; Angeloni, A. S.; Galli, G.; Chiellini, E. *Macromolecules* **1992**, *25*, 5901.

(8) (a) Griffin, A. C.; Havens, S. J. *J. Polym. Sci., Polym. Phys. Ed.* **1981**, *19*, 951. (b) Griffin, A. C.; Britt, T. R. *J. Am. Chem. Soc.* **1981**, *103*, 4957. (c) Sigaud, G.; Yoon, D. Y.; Griffin, A. C. *Macromolecules* **1983**, *16*, 875. (d) Griffin, A. C.; Samulski, E. T. *J. Am. Chem. Soc.* **1985**, *107*, 2975. (e) Blumstein, R. B.; Poliks, M. D.; Stickles, E. M.; Blumstein, A.; Volino, F. *Mol. Cryst. Liq. Cryst.* **1985**, *129*, 375. (f) Toriumi, H.; Furuya, H.; Abe, A. *Polym. J.* **1985**, *17*, 895. (g) Furuya, H.; Asahi, K.; Abe, A. *Polym. J.* **1986**, *18*, 779. (h) Jin, J.-I.; Oh, H. T.; Park, J. H. *J. Chem. Soc., Perkin Trans. 2* **1986**, 343. (i) Jin, J.-I.; Choi, E. J.; Ryu, S. C.; Lenz, R. W. *Polym. J.* **1986**, *18*, 63. (j) Buglione, J. A.; Roviello, A.; Sirigu, A. *Mol. Cryst. Liq. Cryst.* **1984**, *106*, 169. (k) Roviello, A.; Sirigu, A. *Gazz. Chim. Ital.* **1977**, *107*, 333. (l) Auriemma, F.; Corradini, P.; Roviello, A.; Vacatello, M. *Eur. Polym. J.* **1989**, *25*, 57. (m) For a comprehensive discussion on dimers as models for polymers see Sigaud, G. In *Phase Transitions in Liquid Crystals*; Martelucci, S., Chester, A. N., Eds.; Plenum Press: New York, 1992.

(9) Percec, V.; Kawasumi, M. *Macromolecules* **1991**, *24*, 6318.

(10) Percec, V.; Kawasumi, M. *Macromolecules*, in press.

(11) (a) Percec, V.; Kawasumi, M.; Rinaldi, P. L.; Litman, V. E. *Macromolecules* **1992**, *25*, 3851. (b) Percec, V.; Kawasumi, M. *Adv. Mater.* **1992**, *4*, 572. (c) Percec, V.; Kawasumi, M. *Liq. Cryst.* **1993**, *13*, 83. (d) Percec, V.; Kawasumi, M. *J. Chem. Soc., Perkin Trans. 1*, in press and references cited therein.

(12) Percec, V.; Kawasumi, M. *Macromolecules* **1992**, *25*, 3843.

(13) (a) Gu, D.; Jamieson, A. M.; Kawasumi, M.; Lee, M.; Percec, V. *Macromolecules* **1992**, *25*, 2151. (b) Gu, D.; Jamieson, A. M.; Lee, M.; Kawasumi, M.; Percec, V. *Liq. Cryst.* **1992**, *12*, 961. (c) Yoon, D. Y.; Sigaud, G.; Sherwood, M.; Wade, C.; Percec, V. *Bull. Am. Phys. Soc.* **1992**, *37* (1), 369.

(14) (a) Aneja, R.; Davies, A. P.; Knaggs, J. A. *Tetrahedron Lett.* **1974**, 67.

(15) Zweifel, G.; Brown, H. C. *J. Am. Chem. Soc.* **1964**, *86*, 393.

(16) Tung, L. H., Ed. *Fractionation of Synthetic Polymers*; Mercel Dekker: New York, 1977.

(17) Fox, T. G.; Flory, P. J. *J. Appl. Phys.* **1950**, *21*, 581.